Development of an improved online comprehensive hydrophilic interaction chromatography × reversed-phase ultra-high-pressure liquid chromatography platform for complex multiclass polyphenolic sample analysis

JOURNAL OF SEPARATION SCIENCE

Development of an improved online comprehensive hydrophilic interaction chromatography × reversed-phase ultra-high-pressure liquid chromatography platform for complex multiclass polyphenolic sample analysis

Eduardo Sommella1,2, Omar H. Ismail3,Francesco Pagano1,2,Giacomo Pepe1,2,Carmine Ostacolo4, Giulia Mazzoccanti3,Mariateresa Russo1,Ettore Novellino4, Francesco Gasparrini3 Pietro Campiglia
2, First published: ***28 March 2017***

https://doi.org/10.1002/jssc.201700134
Conflict of interest: The authors declare no conflict of interest.

Abstract

In this study, an improved online comprehensive two-dimensional liquid chromatography platform coupled to tandem mass spectrometry was developed for the analysis of complex polyphenolic samples. A narrowbore hydrophilic interaction chromatography column (150 × 2.0 mm, 3.0 μm, cross-linked diol) was employed in the first dimension, while a reversed-phase column based on monodisperse sub-2 μm fully porous particles (50 × 3.0 mm, 1.9 μm d.p.) with high surface area (410 m^2/g) was employed in the second dimension. The combination of a trapping column modulation interface with the high retentive fully porous monodisperse reversed-phase column in the second dimension resulted in higher peak capacity values (1146 versus 867), increased sensitivity, sharper and more symmetrical peaks in comparison with a conventional loop-based method, with the same analysis time (70 min). The system was challenged against a complex polyphenolic extract of a typical Italian apple cultivar, enabling the simultaneous separation of multiple polyphenolic classes, including oligomeric procyanidins, up to degree of polymerization of 10. Hyphenation with an ion trap time-of-flight mass spectrometer led to the tentative identification of 121 analytes, showing how this platform could be a powerful analytical tool for the accurate profiling of complex polyphenolic samples.

1 INTRODUCTION

The detailed characterization of complex natural samples represents a challenge for separation techniques. These multi-component mixtures can contain hundreds of compounds with different chemical features, in a wide concentration range. The natural matrices are also widely used to formulate nutraceuticals and functional foods. This category of products, sold in pharmaceutical form such as capsules, pills or tablets, usually contain enriched phytochemical extracts from foods, plants and fruits 1. Given the increasing demand for quality assessment and claim substantiation in this market, the existence of analytical techniques to thoroughly characterize the composition of these formulations, appears pivotal. LC–MS/MS is the golden standard for the analysis of complex non-volatile phytochemical samples, and in particular, for polyphenols 2. Although the development of UHPLC has further raised the efficiency of this technique, the separation of complex multi-class polyphenolic samples still remains a bottleneck, thus higher resolving power is required. Online comprehensive 2-DLC (LC × LC) is able to provide higher peak capacity values, and is well suited for the analysis of highly complex samples 3. This technique employs two different separation methods that are combined to yield selectivity and higher resolution. The eluate from the first dimension (^{1}D) is continuously collected and re-injected online into the second dimension (^{2}D) through a modulation unit, which is usually a multiport switching valve. Nevertheless, the online coupling of two chromatographic dimensions is subjected to some restrictions. To adequately sample

^{1}D peaks, the ^{2}D separation cycles must be extremely fast and highly efficient 4. Moreover, the compatibility of mobile phase strength should be taken into account, together with the amount of volume injected in the ^{2}D, to achieve efficient peak focusing on the top of ^{2}D column. Several stationary phase combinations have been developed in online comprehensive LC × LC for the separation of polyphenols, such as normal phase (NP) × RP 5, RP × RP 6 and HILIC × RP 7. HILIC, in which a polar stationary phase is employed in combination with an aqueous/polar organic mobile phase and water plays the role of a stronger eluting solvent, offers a different selectivity compared to RP 8. This is the reason why the coupling of HILIC with RP in LC × LC has been reported to be very promising in terms of orthogonality 9. The main challenge for setting up a HILIC × RP approach is represented by the incompatibility of the mobile phase strength employed in the two dimensions. In fact, the highly organic mobile phase used in HILIC, being stronger eluents in RP, can cause severe peak distortion and loss of retention, strongly impairing the ^{2}D separation 8. A possible solution is the employment of a microbore (1.0 mm internal diameter, i.d) column in the ^{1}D, to inject low volumes onto the ^{2}D column 10. Regarding complex polyphenolic samples, this method has been applied for the separation of grape seed tannins, apple and licorice polyphenols, red wine anthocyanins and algae phlorotannins 11-15. The main drawback of this approach relies on the loss of sensitivity, resulting from both flow-splitting after ^{1}D column and from unsatisfactory peak focusing on the top of ^{2}D column, together with low efficiency in the ^{1}D, since microbore columns are highly affected from extra-column band broadening and overloading. In this work a modified online comprehensive HILIC × RP platform is presented. The novelty of the method lies in the coupling of a trapping-based modulation with a fully porous and monodisperse particles (FPP) 16-18 column in the ^{2}D. The method allows us to overcome the main limitations of loop based HILIC × RP approaches such as poor peak focusing, low peak capacity and sensitivity. The developed platform was applied for the separation of a complex polyphenolic extract of a typical Italian apple variety, and the improvements in comparison with conventional loop and trapping based approaches carried out with ^{2}D core–shell RP columns were also evidenced.

2 MATERIALS AND METHODS

2.1 Chemicals

Ultra-pure water (H_2O) was obtained by a Direct-8 Milli-Q system (Millipore, Milan, Italy), and LC–MS-grade acetonitrile (ACN), LC–MS additives, reagent grade formic acid (HCOOH), acetic acid (CH_3COOH) and filter paper Whatman®540 were all purchased from Sigma–Aldrich (St. Louis, Mo, USA). Standards of phloridzin (phloretin-2-*O*-glucoside), cyanidin-3-*O*-galactoside, quercetin-3-*O*-glucoside, quercetin-3-*O*-galactoside, quercetin-3-*O*-xyloside and isorhamnetin-3-*O*-glucoside were purchased from ExtraSynthese (Lione, France). Standards of (+)-catechin and (−)-epicatechin were purchased from Sigma–Aldrich.

2.2 Sampling and sample preparation

Extraction of polyphenols from Annurca apple variety was performed according to 19 with some modification, detailed description is reported in Supporting material.

2.3 Columns

For HILIC × RP-UHPLC analyses a Luna®HILIC was employed as ^{1}D with geometry (L × I.D): 150 mm × 2.0 mm, 3.0 µm (200 Å) from Phenomenex® (Castel Maggiore, Bologna, Italy), whereas a Titan™C_{18} 50 mm × 3.0 mm, 1.9 µm (80 Å) from Supleco (Bellefonte, PA, USA) was used in the ^{2}D. Moreover, a Kinetex™C_{18} 50 mm × 3.0 mm, 2.6 µm (100 Å) (Phenomenex®) was used for comparison purpose. Two SecurityGuard™ Ultra C_{18} 2 × 4.6 mm (L × I.D) (Phenomenex® Castel Maggiore, Bologna, Italy, AJ0-8768) were employed as trapping columns.

2.4 Instrumentation

Mono-dimensional LC and HILIC × RP-UHPLC analyses were performed on a Shimadzu Nexera (Shimadzu, Milan, Italy), consisting of a CBM-20A controller, four LC–30AD dual-plunger parallel-flow pumps, a DGU-20 A5 degasser, an SPD-M20A PDA detector (equipped with 2.5 µL detector

flow cell volume), a CTO-20AC column oven, and a SIL-30AC autosampler. An additional pump LC–20AT was used to deliver the dilution flow by means of a stainless-steel Tee union, 1/16 in., 0.15 mm bore (Vici-Valco®Houston, TX 77255, USA) installed prior the valve. The two dimensions were connected by an ultra-high-pressure ten-port two-position switching valve with a micro-electric actuator (model FCV-12 AH, 1.034 bar; Shimadzu, Kyoto, Japan), placed inside the column oven and equipped with two 20 µL stainless-steel sampling loops in the loop-based configuration, while two C_{18} pre-columns cartridges 4.6 mm × 2.0 mm, were employed to alternatively trap and elute fractions from ^{1}D to ^{2}D, in the trap-based method. The traps were connected to the valve by Viper capillaries of 10 cm × 0.130 mm I.D (Thermo Fisher Scientific, Milan, Italy). The valve configuration is reported in Fig. 1.
A 35 cm × 0.130 mm i.d. viper capillary was used to connect the autosampler to ^{1}D column (4.6 µL), while a 10 cm × 0.130 mm i.d viper capillary was used to connect the ten-port switching valve with ^{2}D column (1.32 µL). All other connections were 0.130 mm i.d. and kept of the shortest length possible. A total extra-column volume of 28.6 µL was determined injecting toluene by using a zero dead volume union in place of the column. Both dimensions and the switching valve were controlled by the LCMS solution®software (Version 5.54, Shimadzu). The instrument was coupled online with a LCMS-IT-TOF (Shimadzu) equipped with an electrospray source operated in negative mode. The LC × LC data were visualized and elaborated into two and three dimensions using Chromsquare® ver. 1.5.01 software (Chromaleont, Messina, Italy).

2.5 Chromatographic conditions: HILIC × RP-UHPLC–ESI-IT-TOF-MS

^{1}D separation was carried out employing as mobile phases: (A) 0.1% CH_3COOH in H_2O/ACN 80/20 v/v; (B) ACN plus 0.1% CH_3COOH with the following gradient: 0–2 min 99% B, 2–60 min, 99–57% B, 60–70 min, 77–20% B. The flow rate was set to 100 µL/min. Column oven was set to 25°C. 4 µL of extract were injected. The make-up flow was 0.1% CH_3COOH in H_2O v/v, and flow rate prior to the trapping was set to 1 mL/min. For ^{2}D separation mobile phases were: (A) 0.1% CH_3COOH in H_2O *v/v*, (B) ACN plus 0.1% CH_3COOH. The ^{2}D separation was performed with a continuous shifted gradient approach (detailed conditions are reported in supporting material). Flow rate was set to 2.2 mL/min. Column oven was set to 55°C. The modulation time was 45 s, corresponding to an injected volume of 75 µL. PDA detection parameters were: sampling rate 100 Hz, time constant 0.025 s, wavelength 254–500 nm. The system was coupled on-line to a hybrid IT-TOF-MS spectrometer operating in negative ESI, scan speed was ≥10 spectra/s, detailed parameters are reported in supporting material.

3 RESULTS AND DISCUSSION

3.1 Preliminary search of chromatographic conditions in both dimensions: ^{1}D optimization

Monodimensional LC methods are often not capable to resolve complex multiclass polyphenolic samples, given the large differences in chemical behavior of these molecules. Comprehensive HILIC × RP offers superior selectivity thanks to the coupling of two orthogonal separation methods. A growing body of data 11, 20 have evidenced the good performances of HILIC diol-based stationary phases especially for the separation of oligomeric flavan-3-ols. Thus, this stationary phase was selected for the employment in the first dimension. As stated before, all online HILIC × RP approaches for polyphenols are based on the employment of a microbore (1.0 mm I.D) HILIC column in the ^{1}D 11-15. Not to incur in the main limitations of this approach, in particular low efficiency deriving from extracolumn contributions and column overloading, we decided to employ a narrowbore (2.0 mm I.D) column in ^{1}D. In online comprehensive LC × LC the first dimension separation influences both the ^{2}D cycle time and the volume of transferred fractions 3. The last aspect is crucial in a HILIC × RP approach, since injecting large volumes of highly organic solvent causes sample breakthrough and other deleterious effects in ^{2}D 9. The HILIC separation was thus optimized by testing different flow rates (from 0.1 to 0.3 mL/min) and gradients. With a sub-optimal flow rate

of 0.1 mL/min larger peak widths were obtained which facilitated a better sampling of ^{1}D peaks onto the ^{2}D, moreover, a linear gradient that included a short isocratic step at the beginning of ^{1}D analysis improved the retention of early eluting compounds. The effect of varying the injection volume from 1 to 5 µL was considered. A volume of 4 µL was selected, giving the best compromise in terms of peak shape and signal intensity (Fig. S1 and S2). In HILIC the retention is generally opposite to RP and increases with increasing sample polarity 9. The obtained separation were in good accordance with previous HILIC methods for polyphenol separations, with compounds containing more hydroxyl (–OH) groups, such as oligomeric flavan-3-ols, being more retained 21.

3.2 Preliminary search of chromatographic condition in both dimensions: ^{2}D optimization

In on-line comprehensive LC × LC the sampling time is an essential parameter, since the two dimensions are connected, ^{2}D analysis time must be equivalent to the sampling period. Several studies reported that at least 2–4 fractions of each peak should be collected from ^{1}D and transferred in the ^{2}D, to avoid the "undersampling" effect 22. Usually, short (30–50 mm) and high efficiency columns are employed, to provide an adequate sampling of the ^{1}D peaks, together with high resolving power 3. UHPLC conditions are very suitable in ^{2}D, increasing speed and resolution, as shown in a consistent number of applications such as polymers, pharmaceuticals, carotenoids and peptides [23-25,18]. In this work we investigated the performance in the ^{2}D of a short (50 × 3.0 mm, L. × I.D) sub-2 µm fully porous monodisperse Titan^{TM} C-18 column, recently introduced in the market and characterized in detail by Ismail et al. 17. As reported in our previous work 18, this column maintains its efficiency at high linear velocities; this aspect makes it an excellent candidate for ^{2}D of LC × LC where ultra-fast separations are mandatory. The Titan^{TM}C$_{18}$, 1.9 µm column shows also higher retention factors compared to core–shell particle columns, which correlate with the high surface area of this column. This can lead to better peak focusing, which is highly beneficial, especially when transferring solvent with high eluotropic strength, reducing band broadening and peak distortion. Regarding the ^{2}D, the separation was tuned by injecting the entire sample with a fast gradient. Flow rates between 2 and 2.5 mL/min and column temperatures ranging from 45 to 55°C were tested. A flow rate of 2.2 mL/min was selected, which resulted in acceptable backpressure values, whereas the separation was carried out at a temperature of 55°C to further speed the separation, shorten the re-equilibration times, and improve peak shapes of glycosylated flavonoids (peaks eluting from 1.90 and 2.65 in Fig. S3).

3.3 HILIC × RP-UHPLC: loop-based approach

In online LC × LC the sampling time defines the injection volume onto ^{2}D, which is a crucial parameter. Since in HILIC × RP approaches the transfer of low volumes in the ^{2}D is desirable 9, to achieve satisfactory peak focusing, we decided to split the flow rate after the ^{1}D column, keeping constant the ^{1}D flow rate. The benefits deriving from splitting the flow rate after ^{1}D, such as the use of linear velocities close to the optimum and reduced analysis times, have been recently highlighted in LC × LC 26. Two different sampling times (60 and 45 s) were tested for method optimization. A sampling time of 45 s, resulted in the injection of a lower volume (12 µL) into the ^{2}D, and thus was selected. Sampling loops of 20 µL were used due to the fact that loops must be slightly larger than the volume of the fractions being transferred 27, this also allows a dilution of the fraction with ^{2}D mobile phase, to reduce the eluotropic strength prior to the re-injection. The employment of a post ^{1}D dilution flow was not considered on the basis of previous HILIC × RPLC approaches 12-15. The optimized HILIC × RPLC UV-contour plot is depicted in Fig. 2a. Although a promising orthogonality could be appreciated, broad and distorted peaks were obtained, especially glycosylated flavonoids, together with a considerable loss of many minor compounds, which were not detected by both PDA and MS/MS detection (see Fig. 2b). This is most probably associated to the injection of a large volume of stronger mobile phase 12, which caused poor peak focusing and sample breakthrough, despite employing a highly retentive ^{2}D column. Therefore, this approach was unsatisfactory.

3.4 HILIC × RP-UHPLC: Trapping based approach

The coupling of two dimensions employing incompatible mobile phases constitutes one of the main challenges in LC × LC, since the injection in ^{2}D of large mobile phase volumes with high elution strength dramatically impairs separation and sensitivity. Among the possible solutions to solve this problem one is the employment of a trapping columns interface 28. This solution is usually employed in proteomics 29, 30 LC × LC based approaches. In this work sampling loops were replaced by two short C_{18} trapping columns (2 × 4.6 mm). A dilution flow was then applied to lower the ^{1}D mobile phase strength prior to the trapping phase. After different attempts (data not shown), a 1:10 ratio was employed. The same modulation time and injection volume were employed for a direct comparison of the two methods. Either forward-flush or back-flush configuration were used for the trapping columns, resulting in no appreciable differences, excluding backpressure increase in the back-flush mode run to run. Hence to preserve trapping columns integrity and to maintain repeatability, the forward-flush configuration was employed.

In this workflow (see Fig. 1), the analytes are briefly trapped on the two cartridges, allowing their re-concentration, before the elution by the ^{2}D gradient. Hence, the separation occurs on the higher retentive ^{2}D column. In this way, the deleterious effects deriving from the eluotropic strength of ^{1}D effluent are minimized while sensitivity is enhanced, since flow splitting is avoided. Moreover, the second peak-focusing on the monodisperse ^{2}D column allows further band compression, and the reduction of band broadening effects relative to the valve and connections. The resulting 2D UV-contour plot is depicted in Fig. 2b.

As can be clearly observed, sharper and symmetrical peaks were obtained in comparison with the loop-based approach ($4\sigma_{avg\ Trapping}$:0.78 s versus $4\sigma_{avg\ Loop}$: 1.32 s), together with clear improvement of sensitivity, in fact several compounds were detected such as Cumaroylquinic derivatives, Isorhamnetin-3-*O*-rutinoside, Quercetin-3-*O*-rhamnoside, and mostly, a large number of procyanidin isomers with DP ranging from 3 to 10, which were not detected in the loop-based method (and optimal employment of the 2D separation space). At the best of our knowledge, HILIC × RP approaches with trapping columns have been used for the separation of oligonucleotides 31 and, very recently for tristyrylphenol ethoxylate-phosphate (TSP) surfactants 32 to overcome the deleterious effect of ^{1}D mobile phase. No applications of this technique have been reported for polyphenols and never using monodisperse fully porous particle columns as ^{2}D. In fact, different from previous HILIC × RP loop-based and trapping-based approaches carried out with core–shell RP columns as ^{2}D, the employment of a monodisperse fully porous in ^{2}D resulted to be highly beneficial. This important aspect can be better appreciated by Fig. 3 that shows the comparison of the trapping setup employing the monodisperse FPP Titan™C_{18}(3a) and the core–shell Kinetex C_{18} as ^{2}D (3b). As depicted in the expansion of 2D and 3D counter plots, the combination of the two trapping columns with the Titan™C_{18} column sharper peaks were obtained, whereas broader and often tailed peak can be observed with the core–shell ^{2}D Kinetex™. The possible explanation is related to the higher retention of the monodisperse FPP column compared to core–shell particle one, which correlates with the high surface area of this column, resulting in a better peak focusing.

3.5 Performance evaluation of HILIC × RP-UHPLC method

System performance, in terms of peak capacity values, is reported in Table 1. The peak capacity of the HILIC × RP-UHPLC system can be calculated by multiplying the individual peak capacities obtained for the two dimensions, however this value is merely theoretical and should be corrected taking into account both the undersampling effect 26 using Eq. 1 in which β is the correction factor described as

$$\beta = \sqrt{1 + 3.35\left(\frac{^{2}t_c}{1_{\overline{w}}}\right)^2} \quad (1)$$

Where $^{2}t_c$ is ^{2}D cycle time (which is equal to the ^{2}D gradient time, plus the ^{2}D re-equilibration time), and w the average ^{1}D peak width. Moreover, the peak capacity should be corrected taking account the correlations among the solute retention in the two dimensions 25, 33. Finally, a value of 1180 was

obtained for practical peak capacity in the trapping-based approach, whereas, a lower value of 867 was attained for the loop-based approach. For a direct comparison with the only previous HILIC × RP approaches on polyphenols in literature that reported practical peak capacity values 7, 34 we used the reported calculations 25, 26, 34, 35, to better appreciate the improvement of our method. Despite the bin counting method of Gilar 36 has been reported to be effective for orthogonality calculation, the complexity of the matrix makes it difficult to select the number and size of bins. The peak capacity gain of trapping method (+36.1%) mainly derives from a better focusing on the top of the ^{2}D column, with respect to the loop-based configuration. The reported practical peak capacity is higher when compared to previous online comprehensive HILIC × RP loop-based approaches that employed microbore columns in ^{1}D for the separation of polyphenols 7, 34. Furthermore, the performance in ^{2}D of Titan™ column was compared with those of core–shell Kinetex™C_{18} column. For the latter, a lower peak capacity (2Dn_c: 925) was attained. To assess the repeatability, HILIC × RP-UHPLC analyses were run in triplicate, CV% values ≤ 0.1 and 7% for retention time and peak area respectively were obtained by using as control five selected peaks regularly distributed in gradient window (Supporting Information Tables S1 and S2).

3.6 HILIC × RP-UHPLC–IT-TOF: application to apple polyphenols analysis

Apple extracts are characterized by different polyphenolic compounds spanning from simple phenolic acids to large procyanidins oligomers. For this reason we used a typical Italian cultivar, namely Annurca, known to be a rich source of polyphenols 19. The employment of MS/MS is mandatory for identification of compounds in complex mixtures. Tentative identification of 121 compounds was attained through accurate MS and MS/MS spectra, UV absorbance, and with the help of both retention time comparison of available standards and MS database searching. The 2D counter plot with peak assignment is depicted in Fig. 4.

Among the tentatively identified compounds different flavonoid classes were present, the complete list of identified compounds is reported in Table S3. The obtained UV counter plot is highly informative, displaying an ordered and structured elution pattern which is similar to those of comprehensive GC (GC × GC): hydroxycinnamic acids and flavonoid monoglycosides eluting in the first part of the chromatogram. Among them, Isorhamnetin and Kaempferol derivatives, being more hydrophobic, elute earlier than quercetin derivatives in HILIC, whereas flavonol diglycosides are more retained. Lastly, larger oligomeric procyanidins elute in the final part of 2D counter plot. In comparison with a previous 1D-LC method, the present method allowed the identification of 83 compounds more than a previous 1D-LC approach 20, in a single analytical run, especially belonging to the procyanidin oligomers and flavonol glycosides. With respect to all 1D-LC–MS approaches on this variety 20, 37, oligomers up to DP 10 were detected for the first time by this approach. Double and triple charged MS spectra of nonamer, *m/z* 1296.7992 $[M–2H]^{2–}$and decamer, *m/z* 960.2147 $[M–3H]^{3–}$ are reported in Fig. S4. Moreover, these oligomers have not been detected in a previous online HILIC × RPLC loop-based method, on different apple varieties 12. Among flavonol glycosides, Peaks 30 (rt:16.98), 30^{a} (rt: 25.33) and $25^{a\text{-}f}$ (rt: 26.79; 28.99; 29.02, 30.53, 31.31, 32.05) were all characterized by similar fragmentation pattern, providing fragment ions at 301 $[Y_0]^–$and 271 $[Y_0\text{-}CHO]^–$ *m/z*, probably resulting from the loss of hexosides and deoxyhexosides: $[M–H–162]^–$, $[M–H–146]^–$and pentosides: $[M–H–132]^–$. These compounds have been tentatively identified as unknown quercetin hexosides and pentosides derivatives, probably positional isomers, and were not found by 1D-LC approaches. In a similar manner peaks 21^{a} and 17^{a} presented the same MS/MS spectrum with a fragment at *m/z* 273, resulting from the loss of respectively one and two hexose moieties of the deprotonated aglycone phloretin ($C_{15}H_{14}O_5$), thus they were tentatively assigned as phloretin and phlordizin unknown derivatives (Fig. S5). In this regard Q-TOF high resolution MS, employing different collision energy (CE), could be a useful tool to elucidate the number and the position of sugar moieties 38. Nevertheless, the employment of faster and more accurate mass spectrometers, such as ion mobility-Q-TOF or Orbitrap-MS devices, could lead to a larger number of identified

compounds, and is currently under evaluation. In the interest of brevity, the complete elucidation of different polyphenolic classes is reported in the supporting information.

4 CONCLUSIONS

This paper reports the development and evaluation of an enhanced online comprehensive HILIC × RP-UHPLC platform coupled to MS/MS for the analysis of complex polyphenolic samples. The combination of a trapping column modulation interface with a high retentive fully porous and monodisperse particle Titan™ C_{18}, 1.9 μm column in ^{2}D allows to overcome the limitation of conventional online HILIC × RP methods carried out employing microbore columns in the ^{1}D and loop-based interfaces. The developed method delivers higher peak capacities and sensitivity, in comparison with a loop-based approach, with the same analysis time. With respect to 1D-LC–MS methods, a higher number of compounds were detected in the Annurca apple extract, extending the knowledge on this apple variety. The coupling with MS/MS make this technique an ideal candidate for fingerprinting studies of complex polyphenolic food samples as well as in nutraceutical formulations.

ACKNOWLEDGMENTS

The authors would like to thank the project 300390PORFARMABIONET – POR FESR Campania 2007/2013 Obiettivo Operativo 2.1-RETE INTEGRATA PER LE BIOTECNOLOGIE APPLICATE A MOLECOLE AD ATTIVITA' FARMACOLOGICA"FARMABIONET".

Supporting Information

Filename		Description
jssc5399-sup-0001-SuppMat.docx	2.8 MB	Supporting Material

REFERENCES

- 1Espín, J. C. M., García-Conesa, T., Tomas-Barberan, F. A., Nutraceuticals: facts and fiction. *Phytochemistry* 2007, 68, 2986– 3008.
- 2Motilva, M. J., Serra, A., Macia, A., Analysis of food polyphenols by ultra high-performance liquid chromatography coupled to mass spectrometry: An overview. *J. Chromatogr. A* 2013, 1292, 66– 82.
- 3Guiochon, G., Marchetti, N., Mriziq, K., Shalliker, R. A., Implementations of two-dimensional liquid chromatography. *J. Chromatogr. A* 2008, 1189, 109– 168.
- 4Dugo, P., Cacciola, F., Kumm, T., Dugo, G., Mondello, L., Comprehensive multidimensional liquid chromatography: theory and applications. *J. Chromatogr. A* 2008, 1184, 353– 368.
- 5Dugo, P., Favoino, O., Luppino, R., Dugo, G., Mondello, L., Comprehensive two-dimensional normal-phase (adsorption)-reversed-phase liquid chromatography. *Anal. Chem.* 2004, 76, 2525– 2530.
- 6Donato, P., Rigano, F., Cacciola, F., Schure, M., Farnetti, S., Russo, M., Dugo, P., Mondello, L., Comprehensive two-dimensional liquid chromatography–tandem mass spectrometry for the simultaneous determination of wine polyphenols and target contaminants. *J. Chromatogr. A* 2016, 1458, 54– 62.
- 7Beelders, T., Kalili, K. M., Joubert, E., de Beer, D., de Villiers, A., Comprehensive two-dimensional liquid chromatographic analysis of rooibos (*Aspalathus linearis*) phenolics. *J. Sep. Sci.* 2012, 35, 1808– 1820.
- 8Jandera, P., Stationary and mobile phases in hydrophilic interaction chromatography: a review. *Anal. Chim. Acta*. 2011, 692, 1– 25.
- 9Jandera, P., Stationary phases for hydrophilic interaction chromatography, their characterization and implementation into multidimensional chromatography concepts. *J. Sep. Sci.* 2008, 31, 1421– 1437.
- 10Jandera, P., Hajek, T., Stankova, M., Vynuchalova, K., Cesla, P., Optimization of comprehensive two-dimensional gradient chromatography coupling in-line hydrophilic interaction and reversed phase liquid chromatography. *J. Chromatogr. A* 2012, 1268, 91– 101.

- 11Kalili, K. M., Vestner, J., Stander, M. A., de Villiers, A., Toward unraveling grape tannin composition: application of online hydrophilic interaction chromatography × reversed-phase liquid chromatography-time-of-flight mass spectrometry for grape seed analysis. *Anal. Chem.* 2013, 85, 9107– 9115.
- 12Montero, L., Herrero, M., Ibáñez, E., Cifuentes, A., Profiling of phenolic compounds from different apple varieties using comprehensive two-dimensional liquid chromatography. *J. Chromatogr. A* 2013, 1313, 275– 283.
- 13Montero, L., Ibáñez, E., Russo, M., di Sanzo, R., Rastrelli, L., Piccinelli, A. L., Celano, R., Cifuentes, A., Herrero, M., Metabolite profiling of licorice (*Glycyrrhiza glabra*) from different locations using comprehensive two-dimensional liquid chromatography coupled to diode array and tandem mass spectrometry detection. *Anal. Chim. Acta.* 2016, 913, 145– 159.
- 14Chandre Willemse, M., Stander, M. A., Vestner, J., Tredoux, A. G. J., de Villiers, A., Comprehensive two-dimensional hydrophilic interaction chromatography (HILIC)× reversed-phase liquid chromatography coupled to high-resolution mass spectrometry (RP-LC-UV-MS) analysis of anthocyanins and derived pigments in red wine. *Anal. Chem.* 2015, 87, 12006– 12015.
- 15Montero, L., Herrero, M., Ibáñez, E., Cifuentes, A., Separation and characterization of phlorotannins from brown algae Cystoseira abies-marina by comprehensive two-dimensional liquid chromatography. *Electrophoresis* 2014, 35, 1644– 1651.
- 16Catani, M., Ismail, O. H., Cavazzini, A., Ciogli, A., Villani, C., Pasti, L., Bergantin, C., Cabooter, D., Desmet, G., Gasparrini, F., Bell, D. S., Rationale behind the optimum efficiency of columns packed with new 1.9 μm fully porous particles of narrow particle size distribution. *J. Chromatogr. A* 2016, 1454, 78– 85.
- 17Ismail, O. H., Catani, M., Pasti, L., Cavazzini, A., Ciogli, A., Villani, C., Kotoni, D., Gasparrini, F., Bell, D. S., Experimental evidence of the kinetic performance achievable with columns packed with the new 1.9 μm fully porous particles Titan C18. *J. Chromatogr. A* 2016, 1454, 86– 92.
- 18Sommella, E., Pepe, G., Ventre, G., Pagano, F., Manfra, M., Pierri, G., Ismail, O., Ciogli, A., Campiglia, P., Evaluation of two sub-2 μm stationary phases, core-shell and totally porous monodisperse, in the second dimension of on-line comprehensive two dimensional liquid chromatography, a case study: separation of milk peptides after expiration date. *J. Chromatogr. A* 2015, 1375, 54– 61.
- 19Tenore, G. C., Campiglia, P., Stiuso, P., Ritieni, A., Novellino, E., Nutraceutical potential of polyphenolic fractions from Annurca apple (*M. pumila* Miller cv Annurca). *Food Chem.* 2013, 140, 614– 622.
- 20Sommella, E., Pepe, G., Pagano, F., Ostacolo, C., Tenore G., C., Russo M., T., Novellino, E., Manfra, M., Campiglia, P., Detailed polyphenolic profiling of Annurca apple (M. pumila Miller cv Annurca) by a combination of RP-UHPLC and HILIC, both hyphenated to IT-TOF mass spectrometry. *Food Res. Int.* 2015, 76, 466– 477.
- 21Yanagida, A., Murao, H., Ohnishi-Kameyama, M., Yamakawa, Y., Shoji, A., Tagashira, M., Kanda, T., Shindo, H., Shibusawa, Y., Retention behavior of oligomeric proanthocyanidins in hydrophilic interaction chromatography. *J. Chromatogr. A* 2007, 1143, 153– 161.
- 22Murphy, R. E., Schure, M. R., Foley, J. P., Effect of sampling rate on resolution in comprehensive two-dimensional liquid chromatography. *Anal. Chem.* 1998, 70, 1585– 1594.
- 23Uliyanchenko, E., Cools, P. J. C. H., van der Wal, S., Schoenmakers, P. J., Comprehensive two-dimensional ultrahigh-pressure liquid chromatography for separations of polymers. *Anal. Chem.* 2012, 84, 7802– 7809.
- 24Huidobro, A. L., Pruim, P., Schoenmakers, P. J., Barbas, C., Ultra rapid liquid chromatography as second dimension in a comprehensive two-dimensional method for the

screening of pharmaceutical samples in stability and stress studies. *J. Chromatogr. A* 2008, 1190, 182– 190.

- 25Cacciola, F., Donato, P., Giuffrida, D., Torre, G., Dugo, P., Mondello, L., Ultra high pressure in the second dimension of a comprehensive two-dimensional liquid chromatographic system for carotenoid separation in red chili peppers. *J. Chromatogr. A* 2012, 1255, 244– 251.
- 26Filgueira, M. R., Huang, Y., Witt, K., Castells, C., Carr, P. W., Improving peak capacity in fast on-line comprehensive two-dimensional liquid chromatography with post first dimension flow-splitting. *Anal. Chem.* 2011, 83, 9531– 9539.
- 27Van der Horst, A., Schoenmakers, P. J., Comprehensive two-dimensional liquid chromatography of polymers. *J. Chromatogr. A* 2003, 1000, 693– 709.
- 28Wilson, S. R., Jankowski, M., Pepaj, M., Mihailova, A., Boix, F., Vivo Truyols, G., Lundanes, E., Greibrokk, T., 2D LC separation and determination of bradykinin in rat muscle tissue dialysate with on-line SPE-HILIC-SPE-RP-MS. *Chromatographia* 2007, 66, 469– 474.
- 29Liu, H., Finch, J. W., Luongo, J. A., Li, G. Z., Gebler, J. C., Development of an online two-dimensional nano-scale liquid chromatography/mass spectrometry method for improved chromatographic performance and hydrophobic peptide recovery. *J. Chromatogr. A* 2006, 1135, 43– 51.
- 30Vonk, R. J., Gargano, A. F. G., Davydova, E., Dekker, H. L., Eeltink, S., de Koning, L. J., Schoenmakers, P. J., Comprehensive two-dimensional liquid chromatography with stationary-phase-assisted modulation coupled to high-resolution mass spectrometry applied to proteome analysis of saccharomyces cerevisiae. *Anal. Chem.* 2015, 87, 5387– 5394.
- 31Li, Q., Lynen, F., Wang, J., Li, H., Xu, G., Sandra, P., Comprehensive hydrophilic interaction and ion-pair reversed-phase liquid chromatography for analysis of di- to deca-oligonucleotides. *J. Chromatogr. A* 2012, 1255, 237– 243.
- 32Gargano, A. F. G., Duffin, M., Navarro, P., Schoenmakers, P. J., Reducing dilution and analysis time in online comprehensive two-dimensional liquid chromatography by active modulation. *Anal. Chem.* 2016, 88, 1785– 1793.
- 33Liu, Z., Patterson, D. G. Jr., Geometric approach to factor analysis for the estimation of orthogonality and practical peak capacity in comprehensive two-dimensional separations. *Anal. Chem.* 1995, 67, 3840– 3845.
- 34Montero, L., Herrero, M., Prodanov, M., Ibáñez, E., Cifuentes, A., Characterization of grape seed procyanidins by comprehensive two-dimensional hydrophilic interaction× reversed phase liquid chromatography coupled to diode array detection and tandem mass spectrometry. *Anal. Bioanal. Chem.* 2013, 405, 4627– 4638.
- 35Kalili, K. M., de Villiers, A., Systematic optimisation and evaluation of on-line, off-line and stop-flow comprehensive hydrophilic interaction chromatography × reversed phase liquid chromatographic analysis of procyanidins. Part II: Application to cocoa procyanidins. *J. Chromatogr. A* 2013, 1289, 69– 79
- 36Gilar, M., Olivova, P., Daly, A. E., Gebler, J. C., Orthogonality of separation in two-dimensional liquid chromatography. *Anal. Chem.* 2005, 77, 6426– 6434.
- 37Mari, A., Tedesco, I., Nappo, A., Russo, G. L., Malorni, A., Carbone, V., Phenolic compound characterisation and antiproliferative activity of ‘‘Annurca” apple, a southern Italian cultivar. *Food Chem.* 2010, 123, 157– 164.
- 38Li, D., Schmitz, O. J., Comprehensive two-dimensional liquid chromatography tandem diode array detector (DAD) and accurate mass QTOF-MS for the analysis of flavonoids and iridoid glycosides in *Hedyotis diffusa*. *Anal Bioanal Chem.* 2015, 407, 231– 240.
- Miriam Pérez-Cova, Romà Tauler, Joaquim Jaumot, Two-Dimensional Liquid Chromatography in Metabolomics and Lipidomics, Metabolomics, 10.1007/978-1-0716-0864-7_3, (25-47), (2021).

- Katia Arena, Francesco Cacciola, Francesca Rigano, Paola Dugo, Luigi Mondello, Evaluation of matrix effect in one-dimensional and comprehensive two-dimensional liquid chromatography for the determination of the phenolic fraction in extra virgin olive oils, Journal of Separation Science, 10.1002/jssc.202000169, **43**, 9-10, (1781-1789), (2020).
- Francesco Cacciola, Francesca Rigano, Paola Dugo, Luigi Mondello, Comprehensive two-dimensional liquid chromatography as a powerful tool for the analysis of food and food products, TrAC Trends in Analytical Chemistry, 10.1016/j.trac.2020.115894, (115894), (2020).
- Kristina Wicht, Mathijs Baert, Ardiana Kajtazi, Sonja Schipperges, Norwin von Doehren, Gert Desmet, André de Villiers, Frederic Lynen, Pharmaceutical impurity analysis by comprehensive two-dimensional temperature responsive × reversed phase liquid chromatography, Journal of Chromatography A, 10.1016/j.chroma.2020.461561, (461561), (2020).
- Katia Arena, Francesco Cacciola, Laura Dugo, Paola Dugo, Luigi Mondello, Determination of the Metabolite Content of Brassica juncea Cultivars Using Comprehensive Two-Dimensional Liquid Chromatography Coupled with a Photodiode Array and Mass Spectrometry Detection, Molecules, 10.3390/molecules25051235, **25**, 5, (1235), (2020).
- Giacomo Pepe, Shara Francesca Rapa, Emanuela Salviati, Alessia Bertamino, Giulia Auriemma, Stella Cascioferro, Giuseppina Autore, Andrea Quaroni, Pietro Campiglia, Stefania Marzocco, Bioactive Polyphenols from Pomegranate Juice Reduce 5-Fluorouracil-Induced Intestinal Mucositis in Intestinal Epithelial Cells, Antioxidants, 10.3390/antiox9080699, **9**, 8, (699), (2020).
- Pedro F. Brandão, Armando C. Duarte, Regina M.B.O. Duarte, Comprehensive multidimensional liquid chromatography for advancing environmental and natural products research, TrAC Trends in Analytical Chemistry, 10.1016/j.trac.2019.05.016, (2019).
- Soraya Chapel, Florent Rouvière, Sabine Heinisch, Pushing the limits of resolving power and analysis time in on-line comprehensive hydrophilic interaction x reversed phase liquid chromatography for the analysis of complex peptide samples, Journal of Chromatography A, 10.1016/j.chroma.2019.460753, (460753), (2019).
  Crossref
- Eduardo Sommella, Emanuela Salviati, Fabrizio Merciai, Michele Manfra, Alessia Bertamino, Francesco Gasparrini, Ettore Novellino, Pietro Campiglia, Online comprehensive hydrophilic interaction chromatography × reversed phase liquid chromatography coupled to mass spectrometry for in depth peptidomic profile of microalgae gastro-intestinal digests, Journal of Pharmaceutical and Biomedical Analysis, 10.1016/j.jpba.2019.112783, (112783), (2019).
- Ji-Liang Cao, Li-Juan Ma, Sheng-Peng Wang, Yun Deng, Yi-Tao Wang, Peng Li, Jian-Bo Wan, Comprehensive qualitative and quantitative analysis of ginsenosides in Panax notoginseng leaves by online two-dimensional liquid chromatography coupled to hybrid linear ion trap Orbitrap mass spectrometry with deeply optimized dilution and modulation system, Analytica Chimica Acta, 10.1016/j.aca.2019.06.040, (2019).
- Katia Arena, Francesco Cacciola, Domenica Mangraviti, Mariosimone Zoccali, Francesca Rigano, Nino Marino, Paola Dugo, Luigi Mondello, Determination of the polyphenolic fraction of Pistacia vera L. kernel extracts by comprehensive two-dimensional liquid chromatography coupled to mass spectrometry detection, Analytical and Bioanalytical Chemistry, 10.1007/s00216-019-01649-w, (2019).
- Eduardo Sommella, Nadia Badolati, Gennaro Riccio, Emanuela Salviati, Sara Bottone, Monica Dentice, Pietro Campiglia, Gian Tenore, Mariano Stornaiuolo, Ettore Novellino, A Boost in Mitochondrial Activity Underpins the Cholesterol-Lowering Effect of Annurca Apple Polyphenols on Hepatic Cells, Nutrients, 10.3390/nu11010163, **11**, 1, (163), (2019).

- Wangjie Lv, Xianzhe Shi, Shuangyuan Wang, Guowang Xu, Multidimensional liquid chromatography-mass spectrometry for metabolomic and lipidomic analyses, TrAC Trends in Analytical Chemistry, 10.1016/j.trac.2018.11.001, (2018).
- Marion Iguiniz, Estelle Corbel, Nicolas Roques, Sabine Heinisch, Quantitative aspects in on-line comprehensive two-dimensional liquid chromatography for pharmaceutical applications, Talanta, 10.1016/j.talanta.2018.11.030, (2018).
- Eduardo Sommella, Francesco Pagano, Emanuela Salviati, Marcello Chieppa, Alessia Bertamino, Michele Manfra, Marina Sala, Ettore Novellino, Pietro Campiglia, Chemical profiling of bioactive constituents in hop cones and pellets extracts by online comprehensive two-dimensional liquid chromatography with tandem mass spectrometry and direct infusion Fourier transform ion cyclotron resonance mass spectrometry, Journal of Separation Science, 10.1002/jssc.201701242, **41**, 7, (1548-1557), (2018).
- Minzhuo Liu, Xueqian Huang, Qi Liu, Miao Chen, Sen Liao, Fawei Zhu, Shuyun Shi, Hua Yang, Xiaoqing Chen, Rapid screening and identification of antioxidants in the leaves of Malus hupehensis using off-line two-dimensional HPLC–UV–MS/MS coupled with a 1,1′-diphenyl-2-picrylhydrazyl assay, Journal of Separation Science, 10.1002/jssc.201800007, **41**, 12, (2536-2543), (2018).
- Léa Marlot, Magali Batteau, Karine Faure, Comparison between centrifugal partition chromatography and preparative liquid chromatography as first dimensions in off-line two-dimensional separation: Application to the isolation of multi-targeted compounds from Edelweiss plant, ELECTROPHORESIS, 10.1002/elps.201800032, **39**, 15, (2011-2019), (2018).
- Chang-liang Yao, Hui-qin Pan, Hui Wang, Shuai Yao, Wen-zhi Yang, Jin-jun Hou, Qing-hao Jin, Wan-ying Wu, De-an Guo, Global profiling combined with predicted metabolites screening for discovery of natural compounds: Characterization of ginsenosides in the leaves of Panax notoginseng as a case study, Journal of Chromatography A, 10.1016/j.chroma.2018.01.040, **1538**, (34-44), (2018).
- Bob W. J. Pirok, Dwight R Stoll, Peter J Schoenmakers, Recent developments in two-dimensional liquid chromatography – Fundamental improvements for practical applications, Analytical Chemistry, 10.1021/acs.analchem.8b04841, (2018).
- Nadia Badolati, Eduardo Sommella, Gennaro Riccio, Emanuela Salviati, Dimitri Heintz, Sara Bottone, Emery Di Cicco, Monica Dentice, Giancarlo Tenore, Pietro Campiglia, Mariano Stornaiuolo, Ettore Novellino, Annurca Apple Polyphenols Ignite Keratin Production in Hair Follicles by Inhibiting the Pentose Phosphate Pathway and Amino Acid Oxidation, Nutrients, 10.3390/nu10101406, **10**, 10, (1406), (2018).
- Yajun Wu, Jingjing Liu, Su Gu, Li Lin, Yingzhuang Chen, Ming Ma, Bo Chen, Orthogonal strategy development using reversed macroporous resin coupled with hydrophilic interaction liquid chromatography for the separation of ginsenosides from ginseng root extract, Journal of Separation Science, 10.1002/jssc.201700487, **40**, 21, (4128-4134), (2017).
- Lidia Montero, Elena Ibáñez, Mariateresa Russo, Luca Rastrelli, Alejandro Cifuentes, Miguel Herrero, Focusing and non-focusing modulation strategies for the improvement of on-line two-dimensional hydrophilic interaction chromatography × reversed phase profiling of complex food samples, Analytica Chimica Acta, 10.1016/j.aca.2017.07.013, **985**, (202-212), (2017).

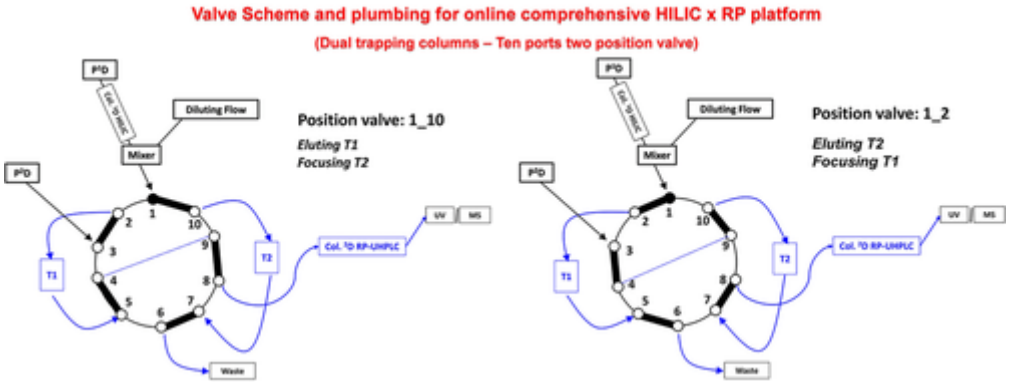

Figure 1 - Schematics of HILIC × RP-UHPLC. The analytes are briefly trapped on the two C_{18} trapping columns. After valve switching the analytes are eluted, re-focused on the top of ^{2}D column and separated.

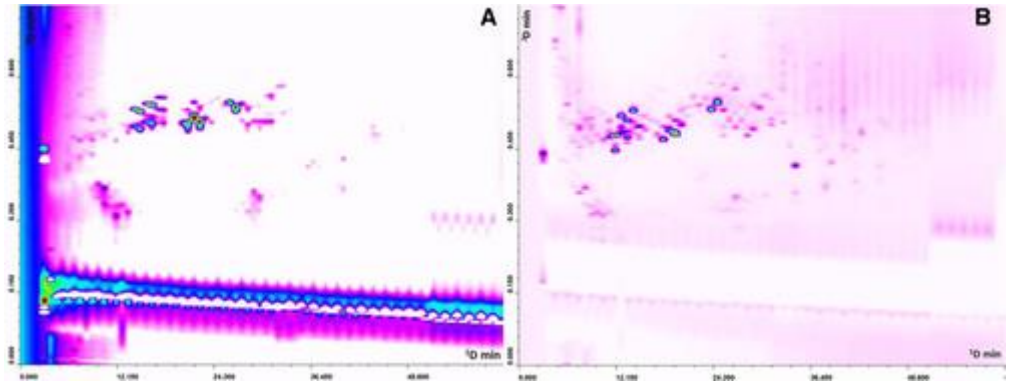

Figure 2 - (a: Left) HILIC × RP-UHPLC separation of the "Annurca" apple polyphenolic extract with loop-based configuration, ^{1}D: Luna® HILIC 150 × 2.0 mm, 3.0 µm (200 Å), ^{2}D: Titan$^{TM}C_{18}$ 50 × 3.0 mm, 1.9 µm (80 Å); (b: Right) HILIC × RP-UHPLC separation of the "Annurca" apple polyphenolic extract with trapping-based configuration. ^{1}D: Luna® HILIC 150 × 2.0 mm, 3.0 µm (200 Å), ^{2}D: Titan$^{TM}C_{18}$ 50 × 3.0 mm, 1.9 µm (80 Å)

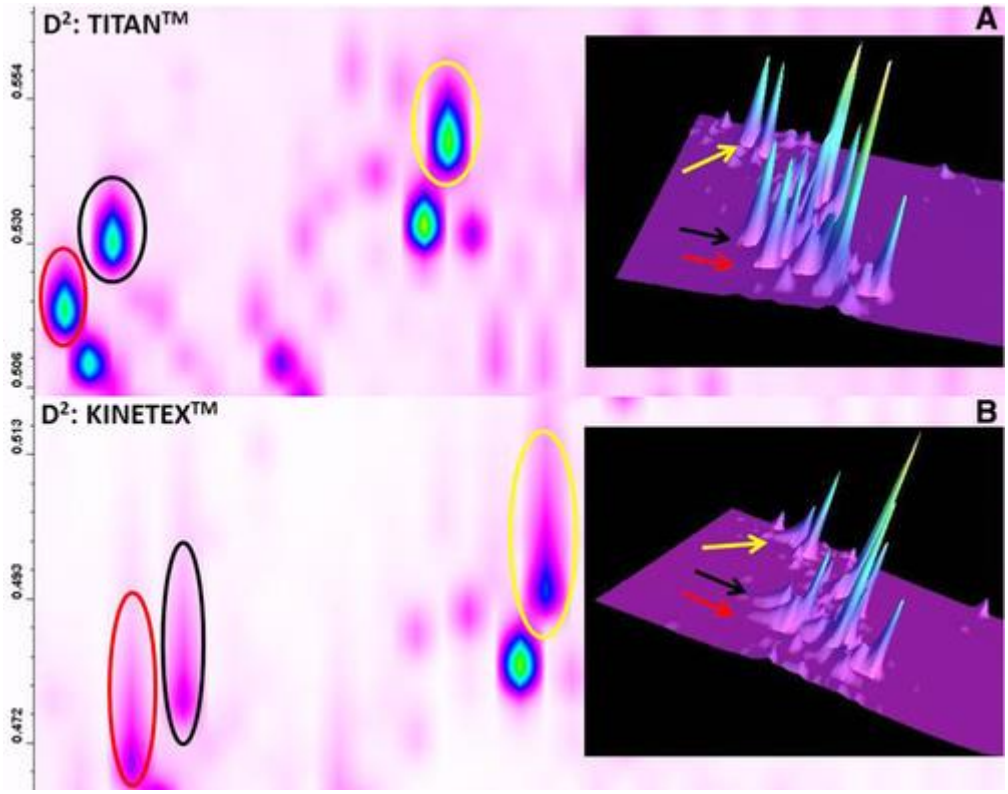

Figure 3 - Expansion of 2D and 3D HILIC × RP-UHPLC plots employing as ^{2}D respectively: Titan^{TM}C$_{18}$ 50 × 3.0 mm, 1.9 µm (top), Kinetex^{TM}C$_{18}$ 50 × 3.0 mm, 2.6 µm (bottom)

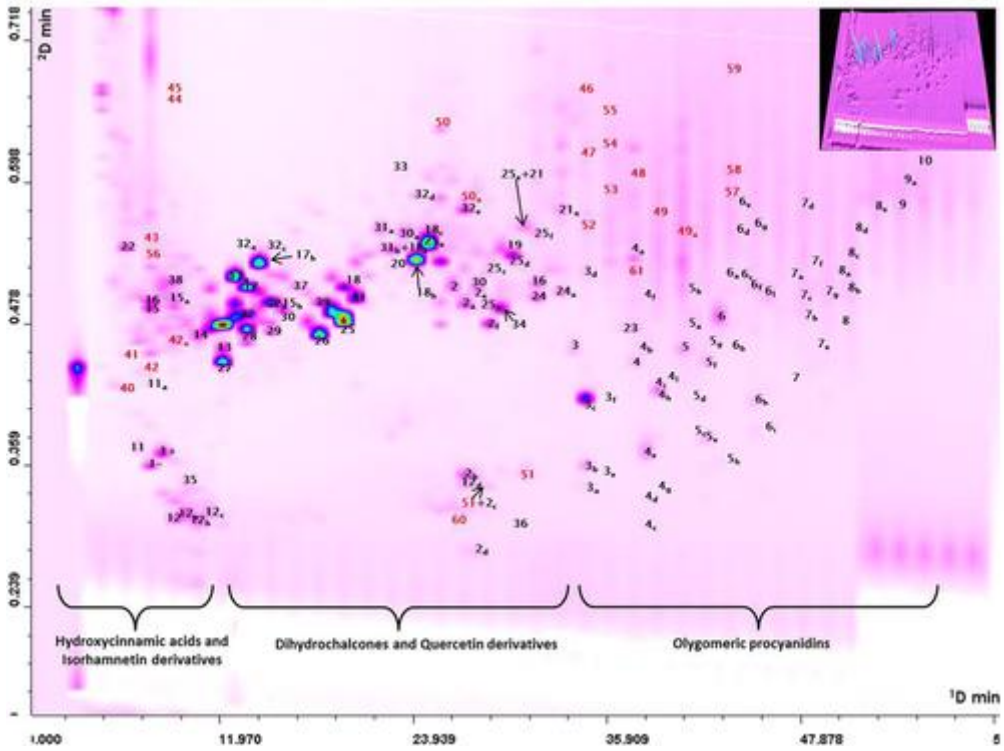

Figure 4 - HILIC × RP-UHPLC 2D counter plot with MS peak assignment, for blob identification please see supporting information table S3 (unknown compounds are marked in red)

Table 1. Performances of HILIC × RP-UHPLC system

PARAMETERS	HILIC × RP-UHPLC (LOOP BASED)	HILIC × RP-UHPLC[C] (TRAPPING BASED)	HILIC × RP-UHPLC[D] (TRAPPING BASED)
^{1}D COLUMN GEOMETRY	Luna® HILIC 150 mm × 2.1 mm, 3.0 µm, (200 Å)	Luna® HILIC 150 mm × 2.1 mm, 3.0 µm, (100 Å)	Luna® HILIC 150 mm × 2.1 mm, 3.0 µm, (100 Å)
^{1}D FLOW RATE	100 µL/min	100 µL/min	100 µL/min
^{1}D COLUMN TEMPERATURE	25°C	25°C	25°C
^{2}D COLUMN GEOMETRY	Titan™ C18 50 × 3.0 mm, 1.9 µm, (80 Å)	Titan™ C18 50 mm × 3.0 mm, 1.9 µm, (80 Å)	Kinetex™ C18 50 mm × 3.0 mm, 2.6 µm (100 Å)
^{2}D FLOW RATE	2.2 mL/min	2.2 mL/min	2.2 mL/min
^{2}D COLUMN TEMPERATURE	55°C	55°C	55°C
^{2}D GRADIENT[A]	Continuously shifted	Continuously shifted	Continuously shifted
ANALYSIS TIME	70 min	70 min	70 min
MODULATION TIME	45 s	45 s	45 s
POST ^{1}D DILUTION FLOW	-	1 mL/min	1 mL/min
THEORETICAL 2D$_{NC}$	1434	1946	1529
PRACTICAL[B] 2D$_{NC}$	867	1180	925

- [a] For detailed conditions see Supporting material.
- [b] Corrected taking into account both undersampling and orthogonality.
- [c] set-up with Titan™ C18 as ^{2}D column.
- [d] set-up with Kinetex™ C18 as ^{2}D column.

Supporting information

Sample extraction

Annurca (*M. pumila* Miller cv Annurca) variety apple fruits were collected in Valle di Maddaloni (Caserta, Italy) in October prior ripening (green peel). Fruits were reddened, following a typical treatment for about 30 days, and then analyzed. Lyophilized peels and flesh (10 g) were treated with 100 mL of 80% methanol (0.5% formic acid) for 24 h at 4 °C to extract polyphenols. After centrifugation, the supernatant was filtered through an Amberlite XAD-2 column packed as follows: resin (10 g; pore size 9 nm; particle size 0.3–1.2 mm; Supelco, Bellefonte, PA, USA) was soaked in methanol, stirred for 10 min and then packed into a glass column (10 × 2 cm). The column was washed with 100 mL of acidified water (pH 2) and 50 mL of deionized water to remove sugar and other polar compounds. The adsorbed compounds were extracted from the resin by elution with 100 mL of methanol, which was evaporated under vacuum. The obtained extract was lyophilized and filtered on 0.45 μm prior analysis.

Ion trap-Time of flight conditions

The HILIC-HPLC × RP-UHPLC system was coupled on-line to a hybrid IT-TOF instrument, the flow rate from LC was split prior of the electrospray (ESI) source by means of a stainless steel tee union (1/16 in., 0.15 mm bore, Valco HX, Texas U.S.) so that approximately 600 μL/min entered into the source. The IT-TOF analyzer was tuned using a standard sample solution of sodium trifluoroacetate. MS detection was operated in negative ionization mode with the following parameters: detector voltage: 1.65 kV, interface voltage: −3.5 kV, curve desolvation line (CDL) temperature: 250 °C, block heater temperature: 250 °C, nebulizing gas flow (N_2): 1.5 L/min, drying gas flow: 12 L/min. Full scan MS data were acquired in the range of 150–1600 m/z, ion accumulation time: 25 ms, ion trap: repeat: 3. MS/MS experiments were conducted in data dependent acquisition, precursor ions were acquired in the range 150–1600 m/z, peak width, 3 Da, ion accumulation time: 50 ms, collision induced dissociation (CID) energy: 50%, collision gas: 50%, ion trap repeat: 1, execution trigger (BPC) intensity at 95% stop level. Dynamic exclusion on: period time 2 s. Scan speed of IT-TOF analyzer was ≥ 10 spectra/s. For the prediction of molecular formulas the "Formula Predictor" software (Shimadzu) was used with the following settings: maximum deviation from mass accuracy: 5 ppm, fragment ion information, and nitrogen rule. The identification of compounds was based on accurate MS and MS/MS spectra, retention time of available standards, and comparison with literature. Moreover the following free on-line databases were consulted: ChemSpider (http://www.chemspider.com), SciFinder Scholar (https://scifinder. cas.org) and Phenol-Explorer (www.phenol-explorer.eu).

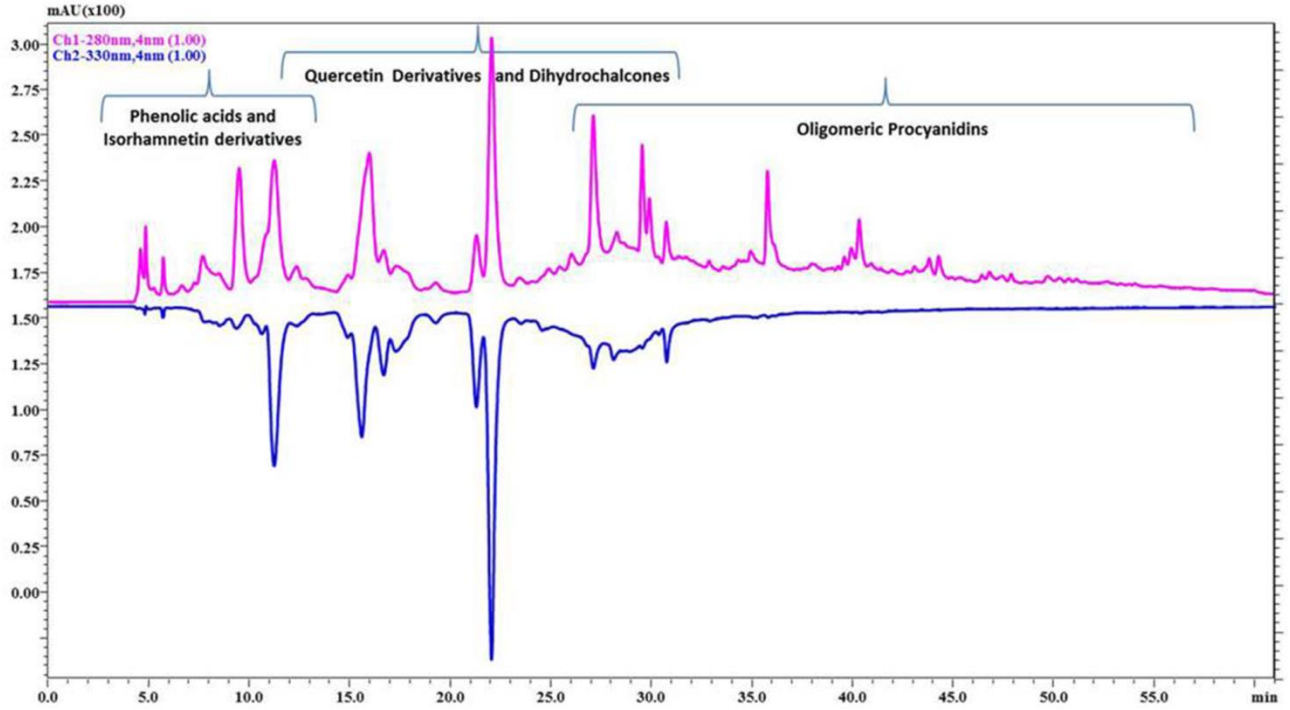

Figure s1: 1D-HILIC-HPLC separation of "Annurca" apple extract. Column Luna HILIC 150 × 2.0 mm, 3.0 μm. Flow rate 0.1 mL/min. Column oven 25 °C. Injection Volume 1 μL.

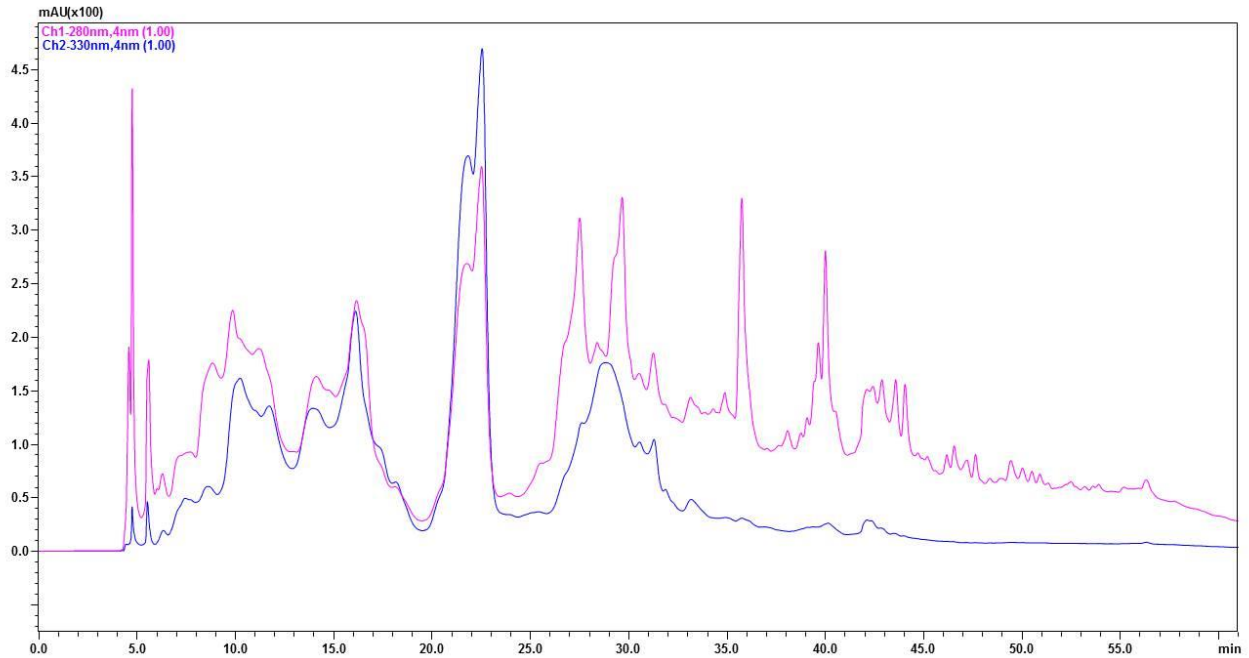

Figure s2: 1D-HILIC-HPLC separation of "Annurca" apple extract. Column Luna HILIC 150 × 2.0 mm, 3.0 μm. Flow rate 0.1 mL/min. Column oven 25 °C. Injection Volume 4 μL.

Blob	^1D		^2D		$^1D + {}^2D$	
	t_r	CV%	t_r	CV%	t_r	CV%
1	7,50	0,0013	0,36	1,0591	7,86	0,0491
2	12,75	0,0008	0,52	0,7677	13,27	0,0303
3	18,00	0,0006	0,48	0,9441	18,48	0,0243
4	24,00	0,0004	0,54	0,7463	24,54	0,0164
5	34,50	0,0003	0,42	1,0238	34,92	0,0124

Table s1: Retention time repeatability of the HILIC-HPLC × RP-UHPLC method

Blob	*Area*	CV %
1	689115,3	7,838
2	4101215	6,242
3	4713920	7,127
4	6014932	2,712
5	2375779	4,951

Table s2: Peak area repeatability of the HILIC-HPLC × RP-UHPLC method

Shifted D^2 gradient

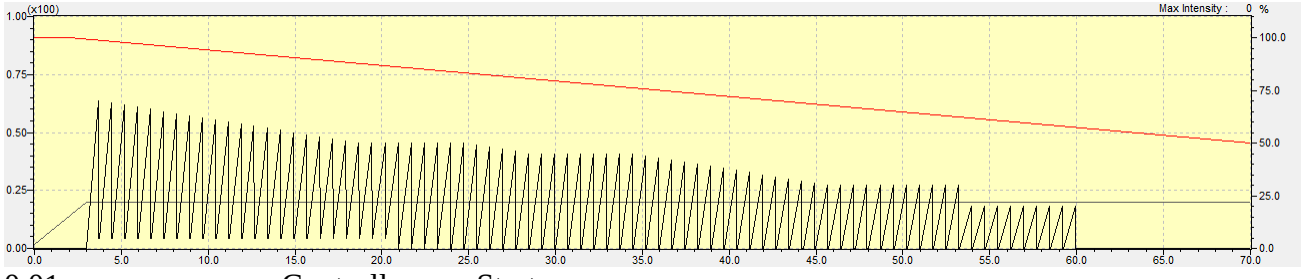

0.01 Controller Start

2.00	Pumps	B.Conc	99
3.00	Pumps	B.Conc3	0
3.00	Oven	CTO.RVR	0
3.00	Pumps	T.Flow3	2.2
3.68	Pumps	B.Conc3	70
3.69	Pumps	B.Conc3	5
3.74	Pumps	B.Conc3	5
3.75	Oven	CTO.RVR	1
4.43	Pumps	B.Conc3	69
4.44	Pumps	B.Conc3	5
4.49	Pumps	B.Conc3	5
4.50	Oven	CTO.RVR	0
5.18	Pumps	B.Conc3	68
5.19	Pumps	B.Conc3	5
5.24	Pumps	B.Conc3	5
5.25	Oven	CTO.RVR	1
5.93	Pumps	B.Conc3	67
5.94	Pumps	B.Conc3	5
5.99	Pumps	B.Conc3	5
6.00	Oven	CTO.RVR	0
6.68	Pumps	B.Conc3	66
6.69	Pumps	B.Conc3	5
6.74	Pumps	B.Conc3	5
6.75	Oven	CTO.RVR	1
7.43	Pumps	B.Conc3	65
7.44	Pumps	B.Conc3	5
7.49	Pumps	B.Conc3	5
7.50	Oven	CTO.RVR	0
8.18	Pumps	B.Conc3	64
8.19	Pumps	B.Conc3	5
8.24	Pumps	B.Conc3	5
8.25	Oven	CTO.RVR	1
8.93	Pumps	B.Conc3	63
8.94	Pumps	B.Conc3	5
8.99	Pumps	B.Conc3	5
9.00	Oven	CTO.RVR	0
9.68	Pumps	B.Conc3	62
9.69	Pumps	B.Conc3	5
9.74	Pumps	B.Conc3	5
9.75	Oven	CTO.RVR	1
10.43	Pumps	B.Conc3	61
10.44	Pumps	B.Conc3	5
10.49	Pumps	B.Conc3	5
10.50	Oven	CTO.RVR	0
11.18	Pumps	B.Conc3	60
11.19	Pumps	B.Conc3	5
11.24	Pumps	B.Conc3	5
11.25	Oven	CTO.RVR	1
11.93	Pumps	B.Conc3	59
11.94	Pumps	B.Conc3	5
11.99	Pumps	B.Conc3	5

12.00	Oven	CTO.RVR	0
12.63	Pumps	B.Conc3	58
12.64	Pumps	B.Conc3	5
12.74	Pumps	B.Conc3	5
12.75	Oven	CTO.RVR	1
13.43	Pumps	B.Conc3	57
13.44	Pumps	B.Conc3	5
13.49	Pumps	B.Conc3	5
13.50	Oven	CTO.RVR	0
14.18	Pumps	B.Conc3	56
14.19	Pumps	B.Conc3	5
14.24	Pumps	B.Conc3	5
14.25	Oven	CTO.RVR	1
14.93	Pumps	B.Conc3	55
14.94	Pumps	B.Conc3	5
14.99	Pumps	B.Conc3	5
15.00	Oven	CTO.RVR	0
15.68	Pumps	B.Conc3	54
15.69	Pumps	B.Conc3	5
15.74	Pumps	B.Conc3	5
15.75	Oven	CTO.RVR	1
16.43	Pumps	B.Conc3	53
16.44	Pumps	B.Conc3	5
16.49	Pumps	B.Conc3	5
16.50	Oven	CTO.RVR	0
17.18	Pumps	B.Conc3	52
17.19	Pumps	B.Conc3	5
17.24	Pumps	B.Conc3	5
17.25	Oven	CTO.RVR	1
17.93	Pumps	B.Conc3	51
17.94	Pumps	B.Conc3	5
17.99	Pumps	B.Conc3	5
18.00	Oven	CTO.RVR	0
18.68	Pumps	B.Conc3	50
18.69	Pumps	B.Conc3	5
18.74	Pumps	B.Conc3	5
18.75	Oven	CTO.RVR	1
19.43	Pumps	B.Conc3	50
19.44	Pumps	B.Conc3	5
19.49	Pumps	B.Conc3	5
19.50	Oven	CTO.RVR	0
20.18	Pumps	B.Conc3	50
20.19	Pumps	B.Conc3	5
20.24	Pumps	B.Conc3	5
20.25	Oven	CTO.RVR	1
20.93	Pumps	B.Conc3	50
20.94	Pumps	B.Conc3	0
20.99	Pumps	B.Conc3	0
21.00	Oven	CTO.RVR	0
21.68	Pumps	B.Conc3	50
21.69	Pumps	B.Conc3	0

21.74	Pumps	B.Conc3	0
21.75	Oven	CTO.RVR	1
22.43	Pumps	B.Conc3	50
22.44	Pumps	B.Conc3	0
22.49	Pumps	B.Conc3	0
22.50	Oven	CTO.RVR	0
23.18	Pumps	B.Conc3	50
23.19	Pumps	B.Conc3	0
23.24	Pumps	B.Conc3	0
23.25	Oven	CTO.RVR	1
23.93	Pumps	B.Conc3	50
23.94	Pumps	B.Conc3	0
23.99	Pumps	B.Conc3	0
24.00	Oven	CTO.RVR	0
24.68	Pumps	B.Conc3	50
24.69	Pumps	B.Conc3	0
24.74	Pumps	B.Conc3	0
24.75	Oven	CTO.RVR	1
25.43	Pumps	B.Conc3	49
25.44	Pumps	B.Conc3	0
25.49	Pumps	B.Conc3	0
25.50	Oven	CTO.RVR	0
26.18	Pumps	B.Conc3	48
26.19	Pumps	B.Conc3	0
26.24	Pumps	B.Conc3	0
26.25	Oven	CTO.RVR	1
26.93	Pumps	B.Conc3	47
26.94	Pumps	B.Conc3	0
26.99	Pumps	B.Conc3	0
27.00	Oven	CTO.RVR	0
27.68	Pumps	B.Conc3	46
27.69	Pumps	B.Conc3	0
27.74	Pumps	B.Conc3	0
27.75	Oven	CTO.RVR	1
28.43	Pumps	B.Conc3	45
28.44	Pumps	B.Conc3	0
28.49	Pumps	B.Conc3	0
28.50	Oven	CTO.RVR	0
29.18	Pumps	B.Conc3	45
29.19	Pumps	B.Conc3	0
29.24	Pumps	B.Conc3	0
29.25	Oven	CTO.RVR	1
29.93	Pumps	B.Conc3	45
29.94	Pumps	B.Conc3	0
29.99	Pumps	B.Conc3	0
30.00	Oven	CTO.RVR	0
30.68	Pumps	B.Conc3	45
30.69	Pumps	B.Conc3	0
30.74	Pumps	B.Conc3	0
30.75	Oven	CTO.RVR	1
31.43	Pumps	B.Conc3	45

31.44	Pumps	B.Conc3	0
31.49	Pumps	B.Conc3	0
31.50	Oven	CTO.RVR	0
32.18	Pumps	B.Conc3	45
32.19	Pumps	B.Conc3	0
32.24	Pumps	B.Conc3	0
32.25	Oven	CTO.RVR	1
32.93	Pumps	B.Conc3	45
32.94	Pumps	B.Conc3	0
32.99	Pumps	B.Conc3	0
33.00	Oven	CTO.RVR	0
33.68	Pumps	B.Conc3	45
33.69	Pumps	B.Conc3	0
33.74	Pumps	B.Conc3	0
33.75	Oven	CTO.RVR	1
34.43	Pumps	B.Conc3	45
34.44	Pumps	B.Conc3	0
34.49	Pumps	B.Conc3	0
34.50	Oven	CTO.RVR	0
35.18	Pumps	B.Conc3	44
35.19	Pumps	B.Conc3	0
35.24	Pumps	B.Conc3	0
35.25	Oven	CTO.RVR	1
35.93	Pumps	B.Conc3	43
35.94	Pumps	B.Conc3	0
35.99	Pumps	B.Conc3	0
36.00	Oven	CTO.RVR	0
36.68	Pumps	B.Conc3	42
36.69	Pumps	B.Conc3	0
36.74	Pumps	B.Conc3	0
36.75	Oven	CTO.RVR	1
37.43	Pumps	B.Conc3	41
37.44	Pumps	B.Conc3	0
37.49	Pumps	B.Conc3	0
37.50	Oven	CTO.RVR	0
38.18	Pumps	B.Conc3	40
38.19	Pumps	B.Conc3	0
38.24	Pumps	B.Conc3	0
38.25	Oven	CTO.RVR	1
38.93	Pumps	B.Conc3	39
38.94	Pumps	B.Conc3	0
38.99	Pumps	B.Conc3	0
39.00	Oven	CTO.RVR	0
39.68	Pumps	B.Conc3	38
39.69	Pumps	B.Conc3	0
39.74	Pumps	B.Conc3	0
39.75	Oven	CTO.RVR	1
40.43	Pumps	B.Conc3	37
40.44	Pumps	B.Conc3	0
40.49	Pumps	B.Conc3	0
40.50	Oven	CTO.RVR	0

41.18	Pumps	B.Conc3	36
41.19	Pumps	B.Conc3	0
41.24	Pumps	B.Conc3	0
41.25	Oven	CTO.RVR	1
41.93	Pumps	B.Conc3	35
41.94	Pumps	B.Conc3	0
41.99	Pumps	B.Conc3	0
42.00	Oven	CTO.RVR	0
42.68	Pumps	B.Conc3	34
42.69	Pumps	B.Conc3	0
42.74	Pumps	B.Conc3	0
42.75	Oven	CTO.RVR	1
43.43	Pumps	B.Conc3	33
43.44	Pumps	B.Conc3	0
43.49	Pumps	B.Conc3	0
43.50	Oven	CTO.RVR	0
44.18	Pumps	B.Conc3	32
44.19	Pumps	B.Conc3	0
44.25	Pumps	B.Conc3	0
44.25	Oven	CTO.RVR	1
44.93	Pumps	B.Conc3	31
44.94	Pumps	B.Conc3	0
44.99	Pumps	B.Conc3	0
45.00	Oven	CTO.RVR	0
45.68	Pumps	B.Conc3	30
45.69	Pumps	B.Conc3	0
45.74	Pumps	B.Conc3	0
45.75	Oven	CTO.RVR	1
46.43	Pumps	B.Conc3	30
46.44	Pumps	B.Conc3	0
46.49	Pumps	B.Conc3	0
46.50	Oven	CTO.RVR	0
47.18	Pumps	B.Conc3	30
47.19	Pumps	B.Conc3	0
47.24	Pumps	B.Conc3	0
47.25	Oven	CTO.RVR	1
47.93	Pumps	B.Conc3	30
47.94	Pumps	B.Conc3	0
47.99	Pumps	B.Conc3	0
48.00	Oven	CTO.RVR	0
48.68	Pumps	B.Conc3	30
48.69	Pumps	B.Conc3	0
48.74	Pumps	B.Conc3	0
48.75	Oven	CTO.RVR	1
49.43	Pumps	B.Conc3	30
49.44	Pumps	B.Conc3	0
49.49	Pumps	B.Conc3	0
49.50	Oven	CTO.RVR	0
50.18	Pumps	B.Conc3	30
50.19	Pumps	B.Conc3	0
50.24	Pumps	B.Conc3	0

50.25	Oven	CTO.RVR	1
50.93	Pumps	B.Conc3	30
50.94	Pumps	B.Conc3	0
50.99	Pumps	B.Conc3	0
51.00	Oven	CTO.RVR	0
51.68	Pumps	B.Conc3	30
51.69	Pumps	B.Conc3	0
51.74	Pumps	B.Conc3	0
51.75	Oven	CTO.RVR	1
52.43	Pumps	B.Conc3	30
52.44	Pumps	B.Conc3	0
52.49	Pumps	B.Conc3	0
52.50	Oven	CTO.RVR	0
53.18	Pumps	B.Conc3	30
53.19	Pumps	B.Conc3	0
53.24	Pumps	B.Conc3	0
53.25	Oven	CTO.RVR	1
53.93	Pumps	B.Conc3	20
53.94	Pumps	B.Conc3	0
53.99	Pumps	B.Conc3	0
54.00	Oven	CTO.RVR	0
54.68	Pumps	B.Conc3	20
54.69	Pumps	B.Conc3	0
54.74	Pumps	B.Conc3	0
54.75	Oven	CTO.RVR	1
55.43	Pumps	B.Conc3	20
55.44	Pumps	B.Conc3	0
55.49	Pumps	B.Conc3	0
55.50	Oven	CTO.RVR	0
56.18	Pumps	B.Conc3	20
56.19	Pumps	B.Conc3	0
56.24	Pumps	B.Conc3	0
56.25	Oven	CTO.RVR	1
56.93	Pumps	B.Conc3	20
56.94	Pumps	B.Conc3	0
56.99	Pumps	B.Conc3	0
57.00	Oven	CTO.RVR	0
57.68	Pumps	B.Conc3	20
57.69	Pumps	B.Conc3	0
57.74	Pumps	B.Conc3	0
57.75	Oven	CTO.RVR	1
58.43	Pumps	B.Conc3	20
58.44	Pumps	B.Conc3	0
58.49	Pumps	B.Conc3	0
58.50	Oven	CTO.RVR	0
59.18	Pumps	B.Conc3	20
59.19	Pumps	B.Conc3	0
59.24	Pumps	B.Conc3	0
59.25	Oven	CTO.RVR	1
59.93	Pumps	B.Conc3	20
59.94	Pumps	B.Conc3	0

59.99	Pumps	B.Conc3	0
60.00	Oven	CTO.RVR	0
70.00	Pumps	B.Conc	50
70.01	Controller	Stop	

Table S3: HILIC-HPLC × RP-UHPLC-IT-TOF elucidation of Annurca apple polyphenolic profile

Peak	2D t_r	Molecular Formula	$[M-H]^-$	[MS/MS]	PDA (nm)	Error (ppm)	Compound
	Hydroxycinnamic acids						
11	7.12	$C_{16}H_{18}O_8$	337.0942	191.0588 $[Quinic\ acid-H]^-$ 163.0441 $[Quinic\ acid-H-CO]^-$	312	-1.19	5-*p*-Cumaroylquinic acid b
11a	7.92	$C_{16}H_{18}O_8$	337.1122	191.0571 $[Quinic\ acid-H]^-$ 163.0348 $[Quinic\ acid-H-CO]^-$	312	-5.34	4-*p*-Coumaroylquinic acid
12	9.31	$C_{16}H_{18}O_9$	353.0846	191.0570 $[Quinic\ acid-H]^-$ 173.0447 $[Quinic\ acid-H-H_2O]^-$	324	-4.16	3'- Caffeolquinic acid
12a	10.70	$C_{16}H_{18}O_9$	353.0873	191.0569 191.0571 $[Quinic\ acid-H]^-$ 173.0400 191.0571 $[Quinic\ acid-H-H_2O]^-$	324	-0.85	5'- Caffeolquinic acid (Chlorogenic Acid)
12b	10.81	$C_{16}H_{18}O_9$	353.0873	191.0569 191.0571 $[Quinic\ acid-H]^-$ 173.0400 191.0571 $[Quinic\ acid-H-H_2O]^-$	324	-0.85	Caffeolquinic acid
12c	11.57	$C_{16}H_{18}O_9$	353.0874	191.0569 191.0571 $[Quinic\ acid-H]^-$ 173.0400 191.0571 $[Quinic\ acid-H-H_2O]^-$	324	-0.87	Caffeolquinic acid
	Dyihydrochalcones						
17	14.02	$C_{21}H_{24}O_{10}$	435.1311	273.0751 $[Y_0]^-$ 167.0375 $[C_8H_7O_4]^-$	284	2.76	Phloridzin
18	21.54	$C_{26}H_{32}O_{14}$	567.1738	273.0748 $[Y_0]^-$	285	1.94	Phloretin-2'-*O*-xylosyl-glucoside
20	24.53	$C_{26}H_{32}O_{15}$	583.1652	289.0695 $[Y_0]^-$ 271.0571 $[Y_0-H2O]^-$	285	-2.23	3-Hydroxyphloretin-2-*O*-xylosyl-glucoside
18a	24.55	$C_{26}H_{32}O_{14}$	567.1738	273.0748 $[Y_0]^-$	285	1.94	Phloretin-2'-*O*-xylosyl-glucoside
18b	26.03	$C_{26}H_{32}O_{14}$	567.1740	273.0748 $[Y_0]^-$	285	1.98	Phloretin-2'-*O*-xylosyl-glucoside
18c	26.80	$C_{26}H_{32}O_{14}$	567.1739	273.0748 $[Y_0]^-$	285	1.95	Phloretin-2'-*O*-xylosyl-glucoside
19	30.54	$C_{26}H_{32}O_{14}$	567.1736	273.0745 $[Y_0]^-$	285	1.93	Phloretin-pentosyl-hexoside
21	31.31	$C_{27}H_{34}O_{15}$	597.1802	273.0742 $[Y_0]^-$	284	-1.51	Phloretin-di-hexoside
	Anthocyanins						
36	32.60	$C_{21}H_{22}O_{12}$	465.1055	285.0392 $[Y_0-2H]^-$	500	3.66	Cyanidin-3-*O*-galactoside

				241.0502 199.0416			
	Flavonols						
22	6.544	$C_{15}H_{10}O_7$	301.0369	151.0089 271.0151[Y_0-CHO]$^-$	255	-17.94	Quercetin
16	7.99	$C_{22}H_{22}O_{11}$	461.1103	315.0485 [Y_0]$^-$ 300.0268 [Y_0-CH_3]$^-$ 271.0236 [Y_0-CH_3-CHO]$^-$	254	1.52	Isorhamnetin-3-*O*-rhamnoside
15	7.991	$C_{21}H_{20}O_{11}$	447.0930	315.0271 [Y_0]$^-$ 300.0271 [Y_0-CH_3]$^-$ 271.0240 [Y_0-CH_3-CHO]$^-$	254	-0.67	Isorhamnetin-3-*O*-pentoside
15a	9.494	$C_{21}H_{20}O_{11}$	447.0934	315.0503 [Y_0]$^-$ 300.0279 [Y_0-CH_3]$^-$ 271.0242 [Y_0-CH_3-CHO]$^-$	254	0.22	Isorhamnetin-3-*O*-pentoside
14	10.97	$C_{22}H_{22}O_{12}$	477.1047	315.0471 [Y_0]$^-$ 300.0299 [Y_0-CH_3]$^-$ 271.0231 [Y_0-CH_3-CHO]$^-$	353	2.30	Isorhamnetin-3-*O*-glucoside
35	10.99	$C_{20}H_{18}O_{10}$	417.0841	285.0388 [Y_0]$^-$ 255.0306 [Y_0-CHO]$^-$	255	0.01	Kaempferol-3-*O*-pentoside
27	12.44	$C_{20}H_{18}O_{11}$	433.0894	301.0338 [Y_0]$^-$ 271.0237 [Y_0-CHO]$^-$	353	0.01	Quercetin-3-*O*-arabinofuranoside (Avicularin)
13	12.45	$C_{22}H_{22}O_{12}$	477.1049	315.0488 [Y_0]$^-$ 300.0282 [Y_0-CH_3]$^-$ 271.0248 [Y_0-CH_3-CHO]$^-$	353	2.31	Isorhamnetin-3-*O*-galactoside
28	13.97	$C_{20}H_{18}O_{11}$	433.0770	301.0335 [Y_0]$^-$ 271.0249 [Y_0-CHO]$^-$	255	1.88	Quercetin-3-*O*-arabinopyranoside (Guajaverin)
32	13.98	$C_{21}H_{20}O_{11}$	447.0931	301.0327 [Y_0]$^-$ 255.0284 [Y_0-CHO-OH]$^-$	254	1.94	Quercetin-3-*O*-rhamnoside (Quercitrin)
29	15.47	$C_{20}H_{18}O_{11}$	433.0773	301.0338 [Y_0]$^-$ 271.0246 [Y_0-CHO]$^-$	353	1.85	Quercetin-3-*O*-xyloside (Reynoutrin)
26	19.98	$C_{21}H_{20}O_{12}$	463.0890	301.0336 [Y_0]$^-$ 271.0241 [Y_0-CHO]$^-$	255	1.73	Quercetin-3-*O*-glucoside (Isoquercetin)
25	20.75	$C_{21}H_{20}O_{12}$	463.0897	301.0338 [Y_0]$^-$	255	3.24	Quercetin-3-*O*-galactoside (Hyperoside)

				271.0242 [Y_0-CHO]$^-$			
31	21.52	$C_{27}H_{28}O_{16}$	607.1286	505.0997 [M-H-$C_4H_8O_3$]$^-$ 463.0867 301.0332 [Y_0]$^-$	351	-3.13	Quercetin-3-[6”-(3-hydroxy-3-methylglutaryl)] β-hexoside
33	24.58	$C_{28}H_{32}O_{16}$	623.1612	315.0499 [Y_0]$^-$ 300.0267 [Y_0-CH_3]$^-$ 271.0240 [Y_0-CH_3-CHO]$^-$	354	-3.37	Isorhamnetin-3-*O*-rutinoside (Narcissin)
34	30.48	$C_{27}H_{30}O_{16}$	609.1465	301.0335 [Y_0]$^-$ 271.0237 [Y_0-CHO]$^-$	353	-1.15	Rutin
24	32.77	$C_{26}H_{28}O_{16}$	595.1308	301.0324 [Y_0]$^-$ 271.0227 [Y_0-CHO]$^-$ 255.0282 [Y_0-CHO-OH]$^-$	269	-1.34	Quercetin-3-*O*-pentosyl hexoside
24$_a$	33.51	$C_{26}H_{28}O_{16}$	595.1297	301.0319 [Y_0]$^-$ 271.0237 [Y_0-CHO]$^-$ 255.0294 [Y_0-CHO-OH]$^-$	269	0.50	Quercetin-3-*O*-pentosyl hexoside
23	36.46	$C_{27}H_{30}O_{17}$	625.1344	463.0799 301.0247 [Y_0]$^-$	255	-9.8	Quercetin-di- hexoside
	Flavanones						
37	17.01	$C_{21}H_{22}O_{10}$	433.1128	271.0611 [Y_0]$^-$ 177.0210 151.0071	278	-2.77	Naringenin-*O*-hexoside
	Flavan-3-ols						
1-	8.61	$C_{15}H_{14}O_6$	289.0719	245.0816 [M-H-C_2H_4O]$^-$	278	-4.57	[-]-Epicatechin
1+	9.36	$C_{15}H_{14}O_6$	289.0702	245.0496 [M-H-C_2H_4O]$^-$	278	-4.57	[+]-Catechin
38	9.51	$C_{25}H_{26}O_{15}$	565.1167	451.1256 289.0687 [Y_0]$^-$ 271.0558 [Y_0-H_2O]$^-$	283	-3.19	Catechin-3-*O*-hexoside derivate
39	20.01	$C_{21}H_{24}O_{11}$	451.1256	289.0705[Y_0]$^-$ 245.0782 [M-H-C_2H_4O]$^-$	285	-5.01	Catechin-3-*O*-hexoside
	Procyanidins						
2	26.76	$C_{30}H_{26}O_{12}$	577.1352	425.0869 [RDA]$^-$	279	-0.69	(Epi) catechin dimer

				407.0754 [RDA-H_2O]$^-$ 289.0697 [QM]$^-$			
2$_a$	27.49	$C_{30}H_{26}O_{12}$	577.1357	425.0869 [RDA]$^-$ 407.0754 [RDA-H_2O]$^-$ 289.0697 [QM]$^-$	282	0.87	(Epi) catechin dimer (isomer)
2$_b$	28.15	$C_{30}H_{26}O_{12}$	577.1345	425.0869 [RDA]$^-$ 407.0754 [RDA-H_2O]$^-$ 289.0697 [QM]$^-$	279	-1.21	(Epi) catechin dimer (isomer)
2$_c$	28.26	$C_{30}H_{26}O_{12}$	577.0772	463.0849 301.0349	279	5.37	(Epi) catechin dimer (isomer)
2$_d$	30.45	$C_{30}H_{26}O_{12}$	577.0772	463.0849 301.0349	279	5.37	(Epi) catechin dimer (isomer)
2$_e$	28.79	$C_{30}H_{26}O_{12}$	577.1338	425.0869 [RDA]$^-$ 407.0754 [RDA-H_2O]$^-$ 289.0697 [QM]$^-$	279	-2.43	(Epi) catechin dimer (isomer)
2$_f$	28.85	$C_{30}H_{26}O_{12}$	577.1339	425.0869 [RDA]$^-$ 407.0754 [RDA-H_2O]$^-$ 289.0697 [QM]$^-$	279	-2.44	(Epi) catechin dimer (isomer)
3	34.27	$C_{45}H_{38}O_{18}$	865.1967	739.1626 [HRF]$^-$ 577.1325 [QM]$^-$ 425.0858 [RDA]$^-$ 407.0728 [RDA-H_2O]$^-$ 287.0550 [QM]$^-$	283	-1.39	Epicatechin trimer (EC-3)
3$_a$	34.95	$C_{45}H_{38}O_{18}$	865.1985	739.1626 [HRF]$^-$ 577.1325 [QM]$^-$ 425.0858 [RDA]$^-$ 407.0728 [RDA-H_2O]$^-$ 287.0550 [QM]$^-$	283	0.01	Epicatechin trimer (EC-3) (isomer)
3$_b$	35.58	$C_{45}H_{38}O_{18}$	865.1968	739.1626 [HRF]$^-$ 577.1325 [QM]$^-$ 425.0858 [RDA]$^-$ 407.0728 [RDA-H_2O]$^-$ 287.0550 [QM]$^-$	283	-1.96	Epicatechin trimer (EC-3) (isomer)

3c	35.61	$C_{45}H_{38}O_{18}$	865.1967	739.1626 $[HRF]^-$ 577.1325 $[QM]^-$ 425.0858 $[RDA]^-$ 407.0728 $[RDA\text{-}H_2O]^-$ 287.0550 $[QM]^-$	283	-2.54	Epicatechin trimer (EC-3) (isomer)
3d	35.67	$C_{45}H_{38}O_{18}$	865.1967	739.1626 $[HRF]^-$ 577.1325 $[QM]^-$ 425.0858 $[RDA]^-$ 407.0728 $[RDA\text{-}H_2O]^-$ 287.0550 $[QM]^-$	283	0.12	Epicatechin trimer (EC-3) (isomer)
3e	36.39	$C_{45}H_{38}O_{18}$	865.1969	739.1626 $[HRF]^-$ 577.1325 $[QM]^-$ 425.0858 $[RDA]^-$ 407.0728 $[RDA\text{-}H_2O]^-$ 287.0550 $[QM]^-$	283	-1.41	Epicatechin trimer (EC-3) (isomer)
3f	36.42	$C_{45}H_{38}O_{18}$	865.1968	739.1626 $[HRF]^-$ 577.1325 $[QM]^-$ 425.0858 $[RDA]^-$ 407.0728 $[RDA\text{-}H_2O]^-$ 287.0550 $[QM]^-$	283	-1.40	Epicatechin trimer (EC-3) (isomer)
4	37.96	$C_{60}H_{50}O_{24}$	576.1231*	865.1856 $[QM]^-$ 739.1675 $[HRF]^-$ 425.0858 $[RDA]^-$ 407.0754 $[RDA\text{-}H_2O]^-$ 577.1297 $[QM]^-$ 575.1172 $[QM]^-$	278	-5.55	Epicatechin tetramer (EC-4)
4a	38.04	$C_{60}H_{50}O_{24}$	576.1242*	865.1856 $[QM]^-$ 739.1675 $[HRF]^-$ 425.0858 $[RDA]^-$ 407.0754 $[RDA\text{-}H_2O]^-$ 577.1297 $[QM]^-$ 575.1172 $[QM]^-$	270	-5.57	Epicatechin tetramer (EC-4) (isomer)

4b	38.70	$C_{60}H_{50}O_{24}$	576.1235*	865.1856 $[QM]^-$ 739.1675 $[HRF]^-$ 425.0858 $[RDA]^-$ 407.0754 $[RDA\text{-}H_2O]^-$ 577.1297 $[QM]^-$ 575.1172 $[QM]^-$	278	-5.21	Epicatechin tetramer (EC-4) (isomer)
4c	39.29	$C_{60}H_{50}O_{24}$	576.1243*	865.1856 $[QM]^-$ 739.1675 $[HRF]^-$ 425.0858 $[RDA]^-$ 407.0754 $[RDA\text{-}H_2O]^-$ 577.1297 $[QM]^-$ 575.1172 $[QM]^-$	279	-4.69	Epicatechin tetramer (EC-4) (isomer)
4d	39.31	$C_{60}H_{50}O_{24}$	576.1240*	865.1856 $[QM]^-$ 739.1675 $[HRF]^-$ 425.0858 $[RDA]^-$ 407.0754 $[RDA\text{-}H_2O]^-$ 577.1297 $[QM]^-$ 575.1172 $[QM]^-$	278	3.22	Epicatechin tetramer (EC-4) (isomer)
4e	39.33	$C_{60}H_{50}O_{24}$	576.1231*	865.1856 $[QM]^-$ 739.1675 $[HRF]^-$ 425.0858 $[RDA]^-$ 407.0754 $[RDA\text{-}H_2O]^-$ 577.1297 $[QM]^-$ 575.1172 $[QM]^-$	278	-5.55	Epicatechin tetramer (EC-4) (isomer)
4f	39.42	$C_{60}H_{50}O_{24}$	1153.2652	865.1856 $[QM]^-$ 739.1675 $[HRF]^-$ 425.0858 $[RDA]^-$ 407.0754 $[RDA\text{-}H_2O]^-$ 577.1297 $[QM]^-$ 575.1172 $[QM]^-$	281	-1.47	Epicatechin tetramer (EC-4) (isomer)
4g	39.43	$C_{60}H_{50}O_{24}$	576.1232*	865.1856 $[QM]^-$ 739.1675 $[HRF]^-$ 425.0858 $[RDA]^-$ 407.0754 $[RDA\text{-}H_2O]^-$	278	-5.56	Epicatechin tetramer (EC-4) (isomer)

				577.1297 $[QM]^-$ 575.1172 $[QM]^-$			
4_h	39.74	$C_{60}H_{50}O_{24}$	576.1230*	865.1856 $[QM]^-$ 739.1675 $[HRF]^-$ 425.0858 $[RDA]^-$ 407.0754 $[RDA\text{-}H_2O]^-$ 577.1297 $[QM]^-$ 575.1172 $[QM]^-$	278	-5.54	Epicatechin tetramer (EC-4) (isomer)
4_i	40.08	$C_{60}H_{50}O_{24}$	576.1231*	865.1856 $[QM]^-$ 739.1675 $[HRF]^-$ 425.0858 $[RDA]^-$ 407.0754 $[RDA\text{-}H_2O]^-$ 577.1297 $[QM]^-$ 575.1172 $[QM]^-$	278	-5.55	Epicatechin tetramer (EC-4) (isomer)
4_l	40.19	$C_{60}H_{50}O_{24}$	576.1235*	865.1856 $[QM]^-$ 739.1675 $[HRF]^-$ 425.0858 $[RDA]^-$ 407.0754 $[RDA\text{-}H_2O]^-$ 577.1297 $[QM]^-$ 575.1172 $[QM]^-$	278	-5.60	Epicatechin tetramer (EC-4) (isomer)
5	41.70	$C_{75}H_{62}O_{30}$	720.1570*	1151.2404 $[QM]^-$ 865.1856 $[QM]^-$ 577.1320 $[QM]^-$ 575.1172 $[QM]^-$ 425.0842 $[RDA]^-$ 407.0783 $[RDA\text{-}H_2O]^-$ 287.0505 $[QM]^-$	270	2.22	Epicatechin pentamer (EC-5)
5_a	41.74	$C_{75}H_{62}O_{30}$	720.1568*	1151.2404 $[QM]^-$ 865.1856 $[QM]^-$ 577.1320 $[QM]^-$ 575.1172 $[QM]^-$ 425.0842 $[RDA]^-$ 407.0783 $[RDA\text{-}H_2O]^-$	278	2.20	Epicatechin pentamer (EC-5) (isomer)

				287.0505 $[QM]^-$			
5b	42.33	$C_{75}H_{62}O_{30}$	720.1571*	1151.2404 $[QM]^-$ 865.1856 $[QM]^-$ 577.1320 $[QM]^-$ 575.1172 $[QM]^-$ 425.0842 $[RDA]^-$ 407.0783 $[RDA\text{-}H_2O]^-$ 287.0505 $[QM]^-$	279	2.62	Epicatechin pentamer (EC-5) (isomer)
5c	42.40	$C_{75}H_{62}O_{30}$	720.1573*	1151.2404 $[QM]^-$ 865.1856 $[QM]^-$ 577.1320 $[QM]^-$ 575.1172 $[QM]^-$ 425.0842 $[RDA]^-$ 407.0783 $[RDA\text{-}H_2O]^-$ 287.0505 $[QM]^-$	278	2.36	Epicatechin pentamer (EC-5) (isomer)
5d	42.47	$C_{75}H_{62}O_{30}$	720.1574*	1151.2404 $[QM]^-$ 865.1856 $[QM]^-$ 577.1320 $[QM]^-$ 575.1172 $[QM]^-$ 425.0842 $[RDA]^-$ 407.0783 $[RDA\text{-}H_2O]^-$ 287.0505 $[QM]^-$	278	2.64	Epicatechin pentamer (EC-5) (isomer)
5e	43.12	$C_{75}H_{62}O_{30}$	720.1570*	1151.2404 $[QM]^-$ 865.1856 $[QM]^-$ 577.1320 $[QM]^-$ 575.1172 $[QM]^-$ 425.0842 $[RDA]^-$ 407.0783 $[RDA\text{-}H_2O]^-$ 287.0505 $[QM]^-$	270	2.22	Epicatechin pentamer (EC-5) (isomer)
5f	43.21	$C_{75}H_{62}O_{30}$	720.1570*	1151.2404 $[QM]^-$ 865.1856 $[QM]^-$ 577.1320 $[QM]^-$ 575.1172 $[QM]^-$ 425.0842 $[RDA]^-$	270	2.22	Epicatechin pentamer (EC-5) (isomer)

				407.0783 [RDA-H_2O]$^-$ 287.0505 [QM]$^-$			
5$_g$	43.87	$C_{75}H_{62}O_{30}$	720.1573*	1151.2404 [QM]$^-$ 865.1856 [QM]$^-$ 577.1320 [QM]$^-$ 575.1172 [QM]$^-$ 425.0842 [RDA]$^-$ 407.0783 [RDA-H_2O]$^-$ 287.0505 [QM]$^-$	270	2.26	Epicatechin pentamer (EC-5) (isomer)
5$_h$	44.0	$C_{75}H_{62}O_{30}$	720.1569*	1151.2404 [QM]$^-$ 865.1856 [QM]$^-$ 577.1320 [QM]$^-$ 575.1172 [QM]$^-$ 425.0842 [RDA]$^-$ 407.0783 [RDA-H_2O]$^-$ 287.0505 [QM]$^-$	270	2.20	Epicatechin pentamer (EC-5) (isomer)
6	44.76	$C_{79}H_{78}O_{44}$	864.1890*	1153.2242 [QM]$^-$ 577.1206 [QM]$^-$ 575.1248 [QM]$^-$ 425.0844 [RDA]$^-$ 407.0707 [RDA-H_2O]$^-$ 287.0629 [QM]$^-$	276	3.74	Epicatechin hexamer (EC-6)
6$_a$	44.80	$C_{79}H_{78}O_{44}$	864.1892*	1153.2242 [QM]$^-$ 577.1206 [QM]$^-$ 575.1248 [QM]$^-$ 425.0844 [RDA]$^-$ 407.0707 [RDA-H_2O]$^-$ 287.0629 [QM]$^-$	279	3.70	Epicatechin hexamer (EC-6) (isomer)
6$_b$	44.83	$C_{79}H_{78}O_{44}$	864.1890*	1153.2242 [QM]$^-$ 577.1206 [QM]$^-$ 575.1248 [QM]$^-$ 425.0844 [RDA]$^-$ 407.0707 [RDA-H_2O]$^-$ 287.0629 [QM]$^-$	276	3.74	Epicatechin hexamer (EC-6) (isomer)

6c	45.42	$C_{79}H_{78}O_{44}$	864.1889*	1153.2242 $[QM]^-$ 577.1206 $[QM]^-$ 575.1248 $[QM]^-$ 425.0844 $[RDA]^-$ 407.0707 $[RDA\text{-}H_2O]^-$ 287.0629 $[QM]^-$	276	3.70	Epicatechin hexamer (EC-6) (isomer)
6d	45.47	$C_{79}H_{78}O_{44}$	864.1891*	1153.2242 $[QM]^-$ 577.1206 $[QM]^-$ 575.1248 $[QM]^-$ 425.0844 $[RDA]^-$ 407.0707 $[RDA\text{-}H_2O]^-$ 287.0629 $[QM]^-$	276	3.76	Epicatechin hexamer (EC-6) (isomer)
6e	45.49	$C_{79}H_{78}O_{44}$	864.1892*	1153.2242 $[QM]^-$ 577.1206 $[QM]^-$ 575.1248 $[QM]^-$ 425.0844 $[RDA]^-$ 407.0707 $[RDA\text{-}H_2O]^-$ 287.0629 $[QM]^-$	276	3.75	Epicatechin hexamer (EC-6) (isomer)
6f	45.54	$C_{79}H_{78}O_{44}$	864.1888*	1153.2242 $[QM]^-$ 577.1206 $[QM]^-$ 575.1248 $[QM]^-$ 425.0844 $[RDA]^-$ 407.0707 $[RDA\text{-}H_2O]^-$ 287.0629 $[QM]^-$	276	3.70	Epicatechin hexamer (EC-6) (isomer)
6g	46.16	$C_{79}H_{78}O_{44}$	864.1890*	1153.2242 $[QM]^-$ 577.1206 $[QM]^-$ 575.1248 $[QM]^-$ 425.0844 $[RDA]^-$ 407.0707 $[RDA\text{-}H_2O]^-$ 287.0629 $[QM]^-$	276	3.74	Epicatechin hexamer (EC-6) (isomer)
6h	46.24	$C_{79}H_{78}O_{44}$	864.1887*	1153.2242 $[QM]^-$ 577.1206 $[QM]^-$ 575.1248 $[QM]^-$ 425.0844 $[RDA]^-$	276	3.69	Epicatechin hexamer (EC-6) (isomer)

				407.0707 [RDA-H_2O]$^-$ 287.0629 [QM]$^-$			
6$_i$	46.89	$C_{79}H_{78}O_{44}$	864.1892*	1153.2242 [QM]$^-$ 577.1206 [QM]$^-$ 575.1248 [QM]$^-$ 425.0844 [RDA]$^-$ 407.0707 [RDA-H_2O]$^-$ 287.0629 [QM]$^-$	276	3.75	Epicatechin hexamer (EC-6) (isomer)
6$_l$	46.99	$C_{79}H_{78}O_{44}$	864.1890*	1153.2242 [QM]$^-$ 577.1206 [QM]$^-$ 575.1248 [QM]$^-$ 425.0844 [RDA]$^-$ 407.0707 [RDA-H_2O]$^-$ 287.0629 [QM]$^-$	276	3.74	Epicatechin hexamer (EC-6) (isomer)
7	47.80	$C_{105}H_{86}O_{42}$	1008.2226*	1153.2242 [QM]$^-$ 865.1958 [QM]$^-$ 739.1429 [HRF]$^-$ 575.1207 [QM]$^-$ 425.0864 [RDA]$^-$ 407.0972 [RDA-H_2O]$^-$	279	-1.37	Epicatechin heptamer (EC-7)
7$_a$	48.45	$C_{105}H_{86}O_{42}$	1008.2227*	1153.2242 [QM]$^-$ 865.1958 [QM]$^-$ 739.1429 [HRF]$^-$ 575.1207 [QM]$^-$ 425.0864 [RDA]$^-$ 407.0972 [RDA-H_2O]$^-$	279	-1.38	Epicatechin heptamer (EC-7) (isomer)
7$_b$	48.50	$C_{105}H_{86}O_{42}$	1008.2230*	1153.2242 [QM]$^-$ 865.1958 [QM]$^-$ 739.1429 [HRF]$^-$ 575.1207 [QM]$^-$ 425.0864 [RDA]$^-$ 407.0972 [RDA-H_2O]$^-$	279	-1.81	Epicatechin heptamer (EC-7) (isomer)
7$_c$	48.54	$C_{105}H_{86}O_{42}$	1008.2232*	1153.2242 [QM]$^-$ 865.1958 [QM]$^-$	279	-1.83	Epicatechin heptamer (EC-7) (isomer)

				739.1429 $[HRF]^-$ 575.1207 $[QM]^-$ 425.0864 $[RDA]^-$ 407.0972 $[RDA-H_2O]^-$			
7d	49.14	$C_{105}H_{86}O_{42}$	1008.2235*	1153.2242 $[QM]^-$ 865.1958 $[QM]^-$ 739.1429 $[HRF]^-$ 575.1207 $[QM]^-$ 425.0864 $[RDA]^-$ 407.0972 $[RDA-H_2O]^-$	279	-1.91	Epicatechin heptamer (EC-7) (isomer)
7e	49.23	$C_{105}H_{86}O_{42}$	1008.2226*	1153.2242 $[QM]^-$ 865.1958 $[QM]^-$ 739.1429 $[HRF]^-$ 575.1207 $[QM]^-$ 425.0864 $[RDA]^-$ 407.0972 $[RDA-H_2O]^-$	279	-1.37	Epicatechin heptamer (EC-7) (isomer)
7f	49.24	$C_{105}H_{86}O_{42}$	1008.2225*	1153.2242 $[QM]^-$ 865.1958 $[QM]^-$ 739.1429 $[HRF]^-$ 575.1207 $[QM]^-$ 425.0864 $[RDA]^-$ 407.0972 $[RDA-H_2O]^-$	279	-1.36	Epicatechin heptamer (EC-7) (isomer)
7g	50	$C_{105}H_{86}O_{42}$	1008.2229*	1153.2242 $[QM]^-$ 865.1958 $[QM]^-$ 739.1429 $[HRF]^-$ 575.1207 $[QM]^-$ 425.0864 $[RDA]^-$ 407.0972 $[RDA-H_2O]^-$	279	-1.39	Epicatechin heptamer (EC-7) (isomer)
8	50.09	$C_{120}H_{98}O_{48}$	1152.2507*	1008.7159 $[HRF-H_2O]^-$ 863.1777 $[QM]^-$ 737.1504 $[HRF]^-$ 575.1162 $[QM]^-$ 449.0860 $[HRF]^-$ 425.0764 $[RDA]^-$	279	- 4.43	Epicatechin octamer

				407.0871 [RDA-H_2O]$^-$			
8$_a$	51.53	$C_{120}H_{98}O_{48}$	1152.2508*	1008.7159 [HRF-H_2O]$^-$ 863.1777 [QM]$^-$ 737.1504 [HRF]$^-$ 575.1162 [QM]$^-$ 449.0860 [HRF]$^-$ 425.0764 [RDA]$^-$ 407.0871 [RDA-H_2O]$^-$	279	- 4.45	Epicatechin octamer (isomer)
8$_b$	52.32	$C_{120}H_{98}O_{48}$	1152.2506*	1008.7159 [HRF-H_2O]$^-$ 863.1777 [QM]$^-$ 737.1504 [HRF]$^-$ 575.1162 [QM]$^-$ 449.0860 [HRF]$^-$ 425.0764 [RDA]$^-$ 407.0871 [RDA-H_2O]$^-$	279	- 4.41	Epicatechin octamer (isomer)
8$_c$	53.02	$C_{120}H_{98}O_{48}$	1152.2510*	1008.7159 [HRF-H_2O]$^-$ 863.1777 [QM]$^-$ 737.1504 [HRF]$^-$ 575.1162 [QM]$^-$ 449.0860 [HRF]$^-$ 425.0764 [RDA]$^-$ 407.0871 [RDA-H_2O]$^-$	279	- 4.60	Epicatechin octamer (isomer)
8$_d$	53.07	$C_{120}H_{98}O_{48}$	1152.2505*	1008.7159 [HRF-H_2O]$^-$ 863.1777 [QM]$^-$ 737.1504 [HRF]$^-$ 575.1162 [QM]$^-$ 449.0860 [HRF]$^-$ 425.0764 [RDA]$^-$ 407.0871 [RDA-H_2O]$^-$	279	- 4.41	Epicatechin octamer (isomer)
8$_e$	53.12	$C_{120}H_{98}O_{48}$	1152.2507*	1008.7159 [HRF-H_2O]$^-$ 863.1777 [QM]$^-$ 737.1504 [HRF]$^-$ 575.1162 [QM]$^-$ 449.0860 [HRF]$^-$	279	- 4.43	Epicatechin octamer (isomer)

				425.0764 [RDA]$^-$ 407.0871 [RDA-H_2O]$^-$			
9	54.58	$C_{135}H_{110}O_{54}$	1296.7783*	863.1916 [QM]$^-$ 575.1260 [QM]$^-$ 449.0851 [HRF]$^-$	278	-5.12	Epicatechin nonamer
9_a	55.3	$C_{135}H_{110}O_{54}$	1296.7785*	863.1912 [QM]$^-$ 575.1261 [QM]$^-$ 449.0849 [HRF]$^-$	278	-5.14	Epicatechin nonamer (isomer)
10	56.12	$C_{150}H_{123}O_{60}$	960.2147*	1153.2321 [QM]$^-$ 575.1083[QM]$^-$ 449.0819 [HRF]$^-$	278	-5.32	Epicatechin decamer
	*Ions Detected as $[M-2H]^{2-}$ and/or $[M-3H]^{3-}$						
	Unknowns						
40	6.42	$C_{27}H_{32}O_{14}$	579.1678	245.0859 289.0655 203.0744 535.1616	279	2.94	unknown

41	6.45	$C_{23}H_{10}O_3$	333.0566	165.0172 301.0356	275 290	2.70	unknown
42	7.89	$C_{16}H_{32}O_9$	367.2014	307.1744 161.0402	268 321	-5.72	unknown
56	8.03	-	485.3231	181.3113 423.3217	260	-	unknown
43	8.05	$C_{44}H_{84}O_{19}$	915.5611	485.3196 423.3299 620.5861 918.5581	264 309	8.41	unknown
44	8.90	$C_{45}H_{96}O_{25}$	517.3135	403.2462 453.3267 292.1993	272 310	17.01	unknown
45	8.95	$C_{32}H_{58}O_{14}$	665.3849	503.3314	309	4.16	unknown
42$_a$	9.418	$C_{16}H_{32}O_9$	367.2014	307.1744 161.0402	268 321	-6.81	unknown
17$_a$	13.26	$C_{21}H_{24}O_{10}$	435.1311	273.0751 $[Y_0]^-$ 167.0375 $[C_8H_7O_4]^-$	284	2.76	Phloridzin unknown derivate
32$_a$	14.78	$C_{21}H_{20}O_{11}$	447.0931	301.0327 $[Y_0]^-$ 255.0284 $[Y_0\text{-CHO-OH}]^-$	254	1.94	Quercetin-hexoside unknown derivate
32$_b$	15.49	$C_{21}H_{20}O_{11}$	447.0931	301.0327 $[Y_0]^-$	254	1.94	

				255.0284 $[Y_0\text{-CHO-OH}]^-$			Quercetin-hexoside unknown derivate
17b	15.52	$C_{21}H_{24}O_{10}$	435.1311	273.0751 $[Y_0]^-$ 167.0375 $[C_8H_7O_4]^-$	284	2.76	Phloridzin unknown derivate
32c	16.29	$C_{21}H_{20}O_{11}$	447.0931	301.0327 $[Y_0]^-$ 255.0284 $[Y_0\text{-CHO-OH}]^-$	254	1.94	Quercetin-hexoside unknown derivate
30	16.98	$C_{20}H_{18}O_{11}$	433.0894	301.0338 $[Y_0]^-$ 271.0237 $[Y_0\text{-CHO}]^-$	353	0.01	Quercetin-hexoside unknown derivate
15b	16.99	$C_{21}H_{20}O_{11}$	447.0930	315.0271 $[Y_0]^-$ 300.0271 $[Y_0\text{-CH}_3]^-$ 271.0240 $[Y_0\text{-CH}_3\text{-CHO}]^-$	254	-0.67	Isorhamnetin-pentoside unknown derivate
31a	23.04	$C_{27}H_{28}O_{16}$	607.1286	505.0997 $[M\text{-H-}C_4H_8O_3]^-$ 463.0867 301.0332 $[Y_0]^-$	351	-3.13	Quercetin-hexoside unknown derivate
31b	24.53	$C_{27}H_{28}O_{16}$	607.1286	505.0997 $[M\text{-H-}C_4H_8O_3]^-$ 463.0867 301.0332 $[Y_0]^-$	351	-3.13	Quercetin-hexoside unknown derivate
30a	25.33	$C_{20}H_{18}O_{11}$	433.0894	301.0338 $[Y_0]^-$ 271.0237 $[Y_0\text{-CHO}]^-$	353	0.01	Quercetin-hexoside unknown derivate
32d	26.08	$C_{21}H_{20}O_{11}$	447.0931	301.0327 $[Y_0]^-$ 255.0284 $[Y_0\text{-CHO-OH}]^-$	254	1.94	Quercetin hexoside unknown derivate
25a	26.79	$C_{21}H_{20}O_{12}$	463.0897	301.0338 $[Y_0]^-$ 271.0242 $[Y_0\text{-CHO}]^-$	255	3.24	Quercetin-hexoside unknown derivate
50	27.64	$C_{46}H_{30}O_8$	709.1861	539.1282 160.3232 289.0695	268	-0.99	unknown
60	27.32	$C_{21}H_{22}O_{12}$	465.1017	285.0409 241.0506 199.0337	255	-4.52	unknown
12d	28.10	$C_{16}H_{18}O_9$	353.0873	191.0569 191.0571 $[\text{Quinic acid-H}]^-$ 173.0400 191.0571 $[\text{Quinic acid-H-}H_2O]^-$	324	-0.85	Caffeolquinic acid unknown derivate

25$_b$	28.99	$C_{21}H_{20}O_{12}$	463.0897	301.0338 $[Y_0]^-$ 271.0242 $[Y_0\text{-CHO}]^-$	255	3.24	Quercetin-hexoside unknown derivate
25$_c$	29.02	$C_{21}H_{20}O_{12}$	463.0897	301.0338 $[Y_0]^-$ 271.0242 $[Y_0\text{-CHO}]^-$	255	3.24	Quercetin-hexoside unknown derivate
32$_e$	29.07	$C_{21}H_{20}O_{11}$	447.0931	301.0327 $[Y_0]^-$ 255.0284 $[Y_0\text{-CHO-OH}]^-$	254	1.94	Quercetin hexoside unknown derivate
50$_a$	29.08	$C_{46}H_{30}O_8$	709.1861	539.1282 160.3232 289.0695	288	-0.99	unknown
51	29.60	$C_{21}H_{22}O_{13}$	481.0940	345.0796 165.0218	268	1.87	unknown
25$_d$	30.53	$C_{21}H_{20}O_{12}$	463.0897	301.0338 $[Y_0]^-$ 271.0242 $[Y_0\text{-CHO}]^-$	255	3.24	Quercetin-hexoside unknown derivate
25$_e$	31.31	$C_{21}H_{20}O_{12}$	463.0897	301.0338 $[Y_0]^-$ 271.0242 $[Y_0\text{-CHO}]^-$	255	3.24	Quercetin-hexoside unknown derivate
51	31.85	$C_{21}H_{22}O_{13}$	481.0940	345.0796 165.0218	268	0.62	unknown
25$_f$	32.05	$C_{21}H_{20}O_{12}$	463.0897	301.0338 $[Y_0]^-$ 271.0242 $[Y_0\text{-CHO}]^-$	255	3.24	Quercetin-hexoside unknown derivate
21$_a$	33.54	$C_{27}H_{34}O_{15}$	597.1802	273.0742 $[Y_0]^-$	284	-1.51	Phloretin-di-hexoside unknown derivate
52	33.68	$C_{61}H_{42}O_{14}$	997.2513	577.1234 407.0681	264	-0.60	unknown
47	35.13	$C_{31}H_{40}O_{10}$	571.2515	263.1437 409.1958	264 301	-5.78	unknown
46	35.20	$C_{44}H_{36}O_{14}$	787.2082	463.0932 625.1440 325.0197	264 301	6.35	unknown
53				685.1747	261		

	36.56	$C_{41}H_{44}O_{20}$	855.2374	155.8249 365.0941 391.0776	275	2.46	unknown
54	36.57	$C_{60}H_{46}O_{24}$	1150.2326	422.3585 161.0952 243.0051	261 275	-4.70	unknown
55	36.65	$C_{36}H_{38}O_{18}$	757.1987	595.1394 475.0851 433.0850	265	0.13	unknown
61	37.99	$C_{58}H_{42}O_{18}$	1025.2264	447.0858 573.1143 609.1131 735.1427	-	-3.32	unknown
48	38.07	$C_{65}H_{58}O_{28}$	642.1466*	287.0613 407.0652 545.1301	263	0.31	unknown
49	39.54	$C_{33}H_{56}O_{18}$	739.3322	577.2554	270	-9.20	unknown
49$_a$	41.05	$C_{33}H_{56}O_{18}$	739.3322	577.2554	278	-9.20	unknown
57	44.05	$C_{49}H_{76}O_{48}$	1432.3510 *	287.0273 398.0626 546.5946	295	0.28	unknown
58	44.10	$C_{77}H_{84}O_{46}$	1744.4078 *	723.1434 577.1436 299.0715	274	-8.95	unknown
59				287.0496	261		

	44.21	$C_{100}H_{86}O_{36}$	1862.4562*	375.0722	274	1.40	unknown

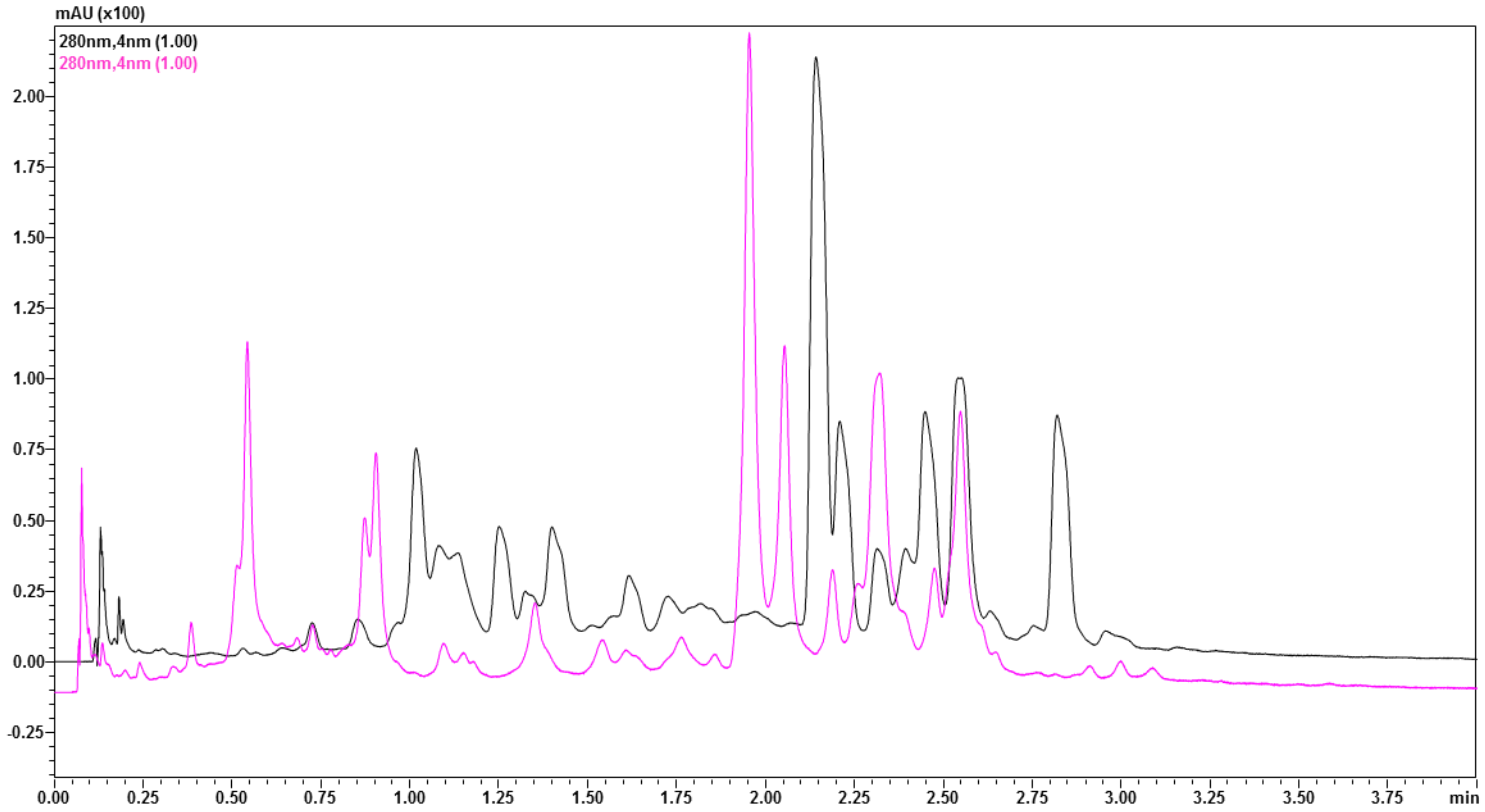

Figure s3 : Comparison of fast gradient elution on Titan^{TM} C18 50 × 3.0 mm, 1.9 µm: pink line: 2.2 mL/min, 55°C, black line: 2.0: mL/min, 50°C

Figure s4: MS and MS/MS spectra of procyanidins with DP 9 (top) and 10 (bottom).

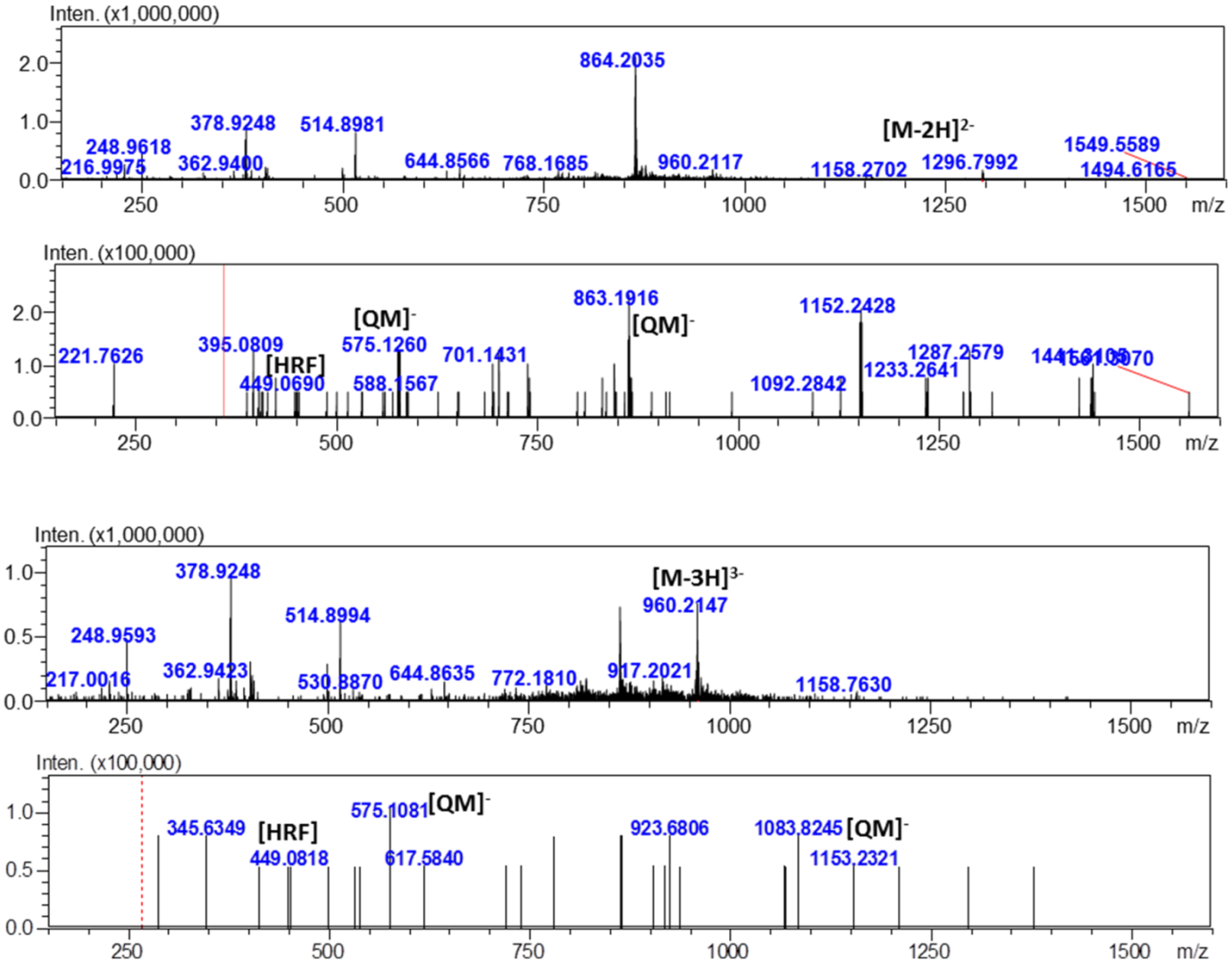
Inten. (x1,000,000)
2.0
1.0
0.0
864.2035
378.9248
514.8981
[M-2H]2-
248.9618
216.9975
362.9400
644.8566
768.1685
960.2117
1158.2702
1296.7992
1549.5589
1494.6165
250
500
750
1000
1250
1500
m/z
Inten. (x100,000)
2.0
1.0
0.0
863.1916
[QM]-
[QM]-
1152.2428
395.0809
575.1260
701.1431
221.7626
[HRF]
449.0690
588.1567
1092.2842
1233.2641
1287.2579
250
500
750
1000
1250
1500
m/z
Inten. (x1,000,000)
1.0
0.5
0.0
378.9248
[M-3H]3-
960.2147
514.8994
248.9593
217.0016
362.9423
530.3870
644.8635
772.1810
917.2021
1158.7630
250
500
750
1000
1250
1500
m/z
Inten. (x100,000)
1.0
0.5
0.0
575.1081
[QM]-
345.6349
[HRF]
923.6806
1083.8245
[QM]-
449.0818
617.5840
1153.2321
250
500
750
1000
1250
1500
m/z

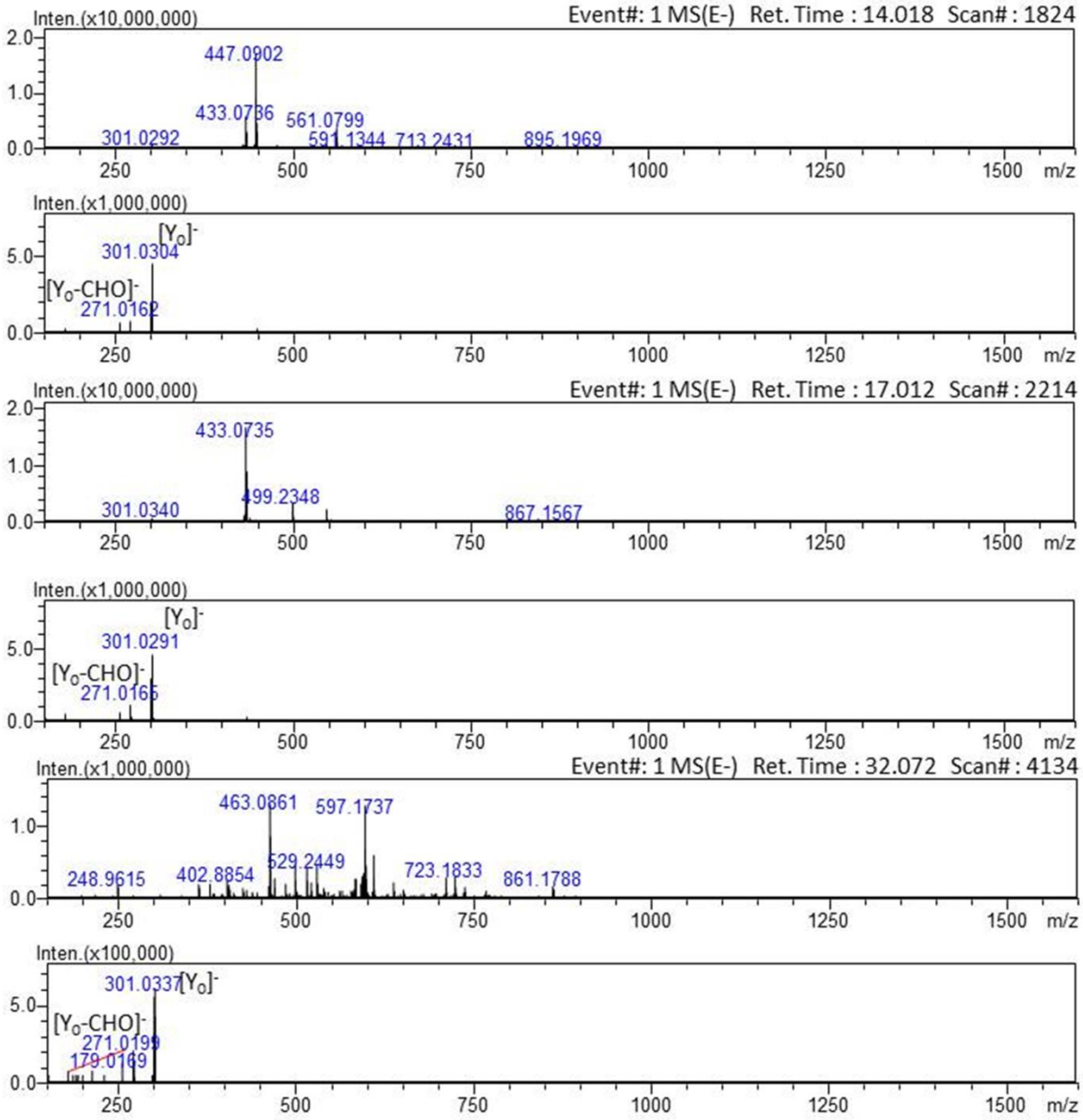
Inten.(x10,000,000)
Event#: 1 MS(E-) Ret. Time : 14.018 Scan# : 1824
447.0902
433.0736
561.0799
301.0292
591.1344
713.2431
895.1969
m/z
Inten.(x1,000,000)
[Y0]-
301.0304
[Y0-CHO]-
271.0162
Inten.(x10,000,000)
Event#: 1 MS(E-) Ret. Time : 17.012 Scan# : 2214
433.0735
499.2348
301.0340
867.1567
Inten.(x1,000,000)
[Y0]-
301.0291
[Y0-CHO]-
271.0165
Inten.(x1,000,000)
Event#: 1 MS(E-) Ret. Time : 32.072 Scan# : 4134
463.0861
597.1737
529.2449
248.9615
402.8854
723.1833
861.1788
Inten.(x100,000)
301.0337
[Y0]-
[Y0-CHO]-
271.0199
179.0169

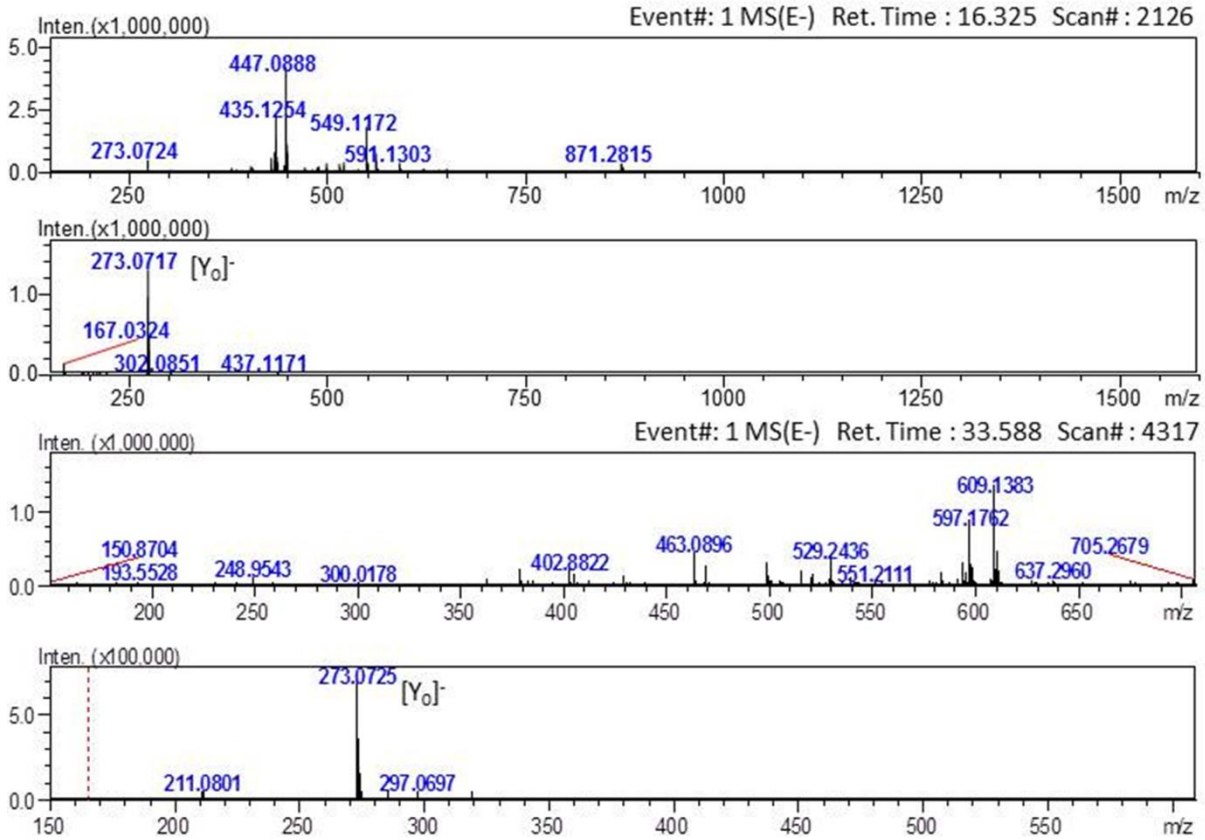

Figure S5: Unknown positional isomers of Quercetin and Phloretin derivatives

MS/MS peak identification

Hydroxycinnamic acids

Hydroxycinnamic acids eluted in the time range from 7.12 to 11.57 min. Compounds 11 and 11_a (rt 7.12, 7.92) were both characterized by MS/MS fragments at m/z 191.0571, of the deprotonated quinic acid moiety, and m/z 163.0348 [quinic acid-HCO]$^-$, and were proposed as 5 and 4-p-coumaroylquinic acid respectively (Fromm, Loos, Bayha, Carle, & Kammerer, 2013). Similarly were compounds 12 and 12_a (rt 9.31, 10.70), so they were tentatively assigned as 3′ isomer caffeoylquinic acid and its 5′ caffeoylquinic acid (chlorogenic acid) (Ramirez-Ambrosi et al., 2013) together with other two isomers 12_b e 12_c (rt 10.81, 11.57).

Dihydrochalcones

Compound 20 (rt 24.53) showed MS/MS fragments at m/z 289.0695 and 271.0571, the first deriving from the sequential loss of a pentose and a hexose moiety, while the second denotes the possible loss of an hydroxyl group, and was tentatively assigned as 3-hydroxyphloretin-2-O-xylosyl-glucoside as reported elsewhere (Alonso-Salces et al., 2004; Ramirez-Ambrosi et al., 2013). Peak 21 (rt 31.31) presented a MS/MS fragment at m/z 273.0742, resulting from the loss of two hexose moieties, of the deprotonated aglycone phloretin ($C_{15}H_{14}O_5$), and was tentatively recognized as phloretin-di-hexoside (Fromm et al., 2013). Peak 18 (rt 21.54) exhibited an intense MS signal and absorbance at 280 nm, showing the fragment at m/z at 273.0748, deriving as for peak 20, from the loss of two sugar moieties, and was tentatively identified as phloretin-2′-O-xylosylglucoside. Similarly, peak 19 (rt 30.54), which was assigned as phloretin-pentosyl-hexoside, other complementary techniques are necessary to confirm this hypothesis, in accordance with previous literature (Ramirez-Ambrosi et al., 2013; Reis, Rai, & Abu-Ghannam, 2012). Last compound of this class, 17 (rt 14.02) with [M-H]$^-$ 435.1311, was easily identified as phloridzin by comparison with standard rt, the loss of 162 amu highlights the presence of glucose, this compound represents one of the most abundant compounds in apples (Fromm, Bayha, Carle, & Kammerer, 2012). Other unknown hexoside isomers were detected (18_a 18_b 18_c rt: 24.55 26.03 26.80).

Anthocyanins

One anthocyanin was detected, even if its absorbance at 500 nm was weak, indicating a low concentration (Garcia-Beneytez, Cabello, & Revilla, 2003). Peak 36 (rt 32.60,) showed ions at m/z 465.1055 and 447.0977 correspond to the adduct [M-2H + H_2O]$^-$ and to [M-2H]$^-$ (Sun, Lin, & Chen, 2012). The fragment ion at m/z 285.0392 [M-2H- 162]$^-$ is charachteristic of the deprotonated aglycone cyanidin ($C_{15}H_{11}O_6$), finally leading, by further comparison with standard retention time, to its identification as cyanidin-3-O-galactoside.

Quercetin derivatives.

Compounds 24 and 24_a (rt 32.77, 33.51) having [M-H]$^-$ at m/z 595.1308 showed the same fragment ion at m/z 301.0324 with molecular formula $C_{15}H_{10}O_7$, probably derived from the sequential loss of a pentose and a hexose, they were tentatively assigned as quercetin-3-O-pentosyl-hexoside derivatives (Oszmianski, Wojdylo, Gorzelany, & Kapusta, 2011). Peak 26 (rt 19.98), showed a fragment ion at m/z 301.0338, of the quercetin aglycone, like peak 25 (rt 20.75) . By comparison with the standard retention time, these compounds were identified as quercetin-3-O-glucoside and quercetin-3-O-galactoside respectively, with the glucoside form that elutes first in HILIC (Kalili & de Villiers, 2009). Peak 34 (rt 30.48), was characterized by an ion at m/z 463.0884 derived from an in source fragmentation and, in the MS/MS spectrum, a fragment at m/z 301.0335 which suggests the loss of a rhamnose and a hexose, and was identified as rutin (Sommella et al., 2013). Peaks 27–32–29 (rt 12.44, 13.98, 15.47) were isobars and lead to same fragments [M-H-132]$^-$, as reported in literature (Schieber, Conrad, Beifuss, & Carle, 2002) and considering the retention time of quercetin-3-O-xyloside standard, they were assigned as quercetin-3-O- arabinofuranoside, 3-O-arabinopyranoside, and 3-O- xyloside respectively. Peak 31 (rt 21.52) showed the ion at m/z 463.0867 which can be attributed to the loss of a methylglutaryl moiety [M-H-144] $^-$, while the ion at m/z 505.0997 to a rearrangement into a 6″ acetate form, leading to the tentative assignment as quercetin-3-O-[6″-(3-hydroxy-3-methylglutaryl)]-β-hexoside, as reported recently in other matrices (Porter,

Van den Bos, Kite, Veitch, & Simmonds, 2012). Peak 32 (rt 13.98), with MS/MS 301.0327, showed a difference of 146 Da, corresponding to the loss of rhamnose, and leading to possible identification as quercetin-3-O-rhamnoside.

Isorhamnetin derivatives.

Peaks 14 and 13 (rt 10.97, 12.45) exhibited the same precursor ion, and their main fragment ions, at m/z 315.0488, with molecular formula $C_{16}H_{12}O_7$, belong to the deprotonated aglycone isorhamnetin, hence, by comparison with the retention time of isorhamnetin-3-O-glucoside standard they were finally tentatively identified as 3-O-glucoside and 3-O- galactoside forms respectively (Schieber, Keller, Streker, Klaiber, & Carle, 2002). Peak 33 (rt 24.58) showed, in a similar manner to rutin, the loss of two sugar moieties, $[M-H-146-162]^-$, identifying the compound as isorhamnetin-3- O-rutinoside in accordance with previous Q-TOF data (Ramirez- Ambrosi et al., 2013). Peaks 15 and 15_a (rt 7.99, 9.49) showed similar fragmentation pattern, with MS/MS fragment ion at m/z 315.0271 and 315.0253 respectively, the difference of 132 Da suggests the loss of a pentose moiety, leading to their tentative identification as isorhamnetin-3-O-pentosides. As for peak 14, the difference of 146 Da points out the loss of rhamnose, and the last eluting peak, 16 (rt 7.99), was finally identified as isorhamnetin-3-Orhamnoside (Alonso-Salces et al., 2004). Only one isorhamnetin derivative was reported in Annurca extract (Mari et al., 2010).

Kaempferol derivatives.

Peak 35 (rt 10.99) showed the MS/MS fragment ions at m/z 285.0839 and 255.0272, the loss of 132 Da revealed the presence of a pentose moiety, this was tentatively identified as kaempferol-3-O-pentoside, in accordance with accurate MSn data (March & Miao, 2004).

Flavanones

Peak 37 (rt 17.01), showed its main fragment ion, at m/z 271.0611, resulting by to the loss of a hexose (162 Da), by literature comparison (Sanchez-Rabaneda et al., 2004), this compound was characterized as naringenin-O-hexoside, and was not reported so far in Annurca extract.

Flavan-3-ols

Peaks 1- and 1+ (rt 8.61, 9.36), were identified by further comparison with the corresponding standards, as (-)-catechin and (+)-epicatechin respectively. MS/MS spectrum of peak 39 (rt 20.01) was characterized by fragments at m/z 289.0705 and 245.0782, the loss of 162 Da can be attributed to a hexose moiety, thus the compound was tentatively identified as catechin-3-O-hexoside. Similarly peak 38, this compound was tentatively identified as unknown catechin- 3-O-hexoside derivative.

Procyanidins

Multiple isomers were detected, spanning from DP 2 to 10. Peaks $2–2_a- 2_b -2_c -2_d -2_e - 2_f$ (rt 26.76, 27.49, 28.15, 28.26, 30.45, 28.79, 28.85) showed similar fragmentation pattern, ions with m/z 289.0767 belong to the monomer (epi)catechin as consequence of quinone methide (QM) cleavage of the inter flavan bond, while fragments at 425.0869 and 407.0754 corresponding to a retro-Diels–Alder (RDA) mechanism $[M-H-152]^-$ and subsequent loss of water respectively. Based on these informations these were tentatively identified as (epi)catechin dimers (Gu et al., 2003). Peaks $3–3_a–3_b–3_c–3_d-3_e-3_f$ (rt 34.27, 34.95, 35.58, 35.61, 35.67, 36.39, 36.42) were all characterized by the fragment at m/z 739.1626, probably resulting from the loss of phloroglucinol unit (heterocyclic ring fission, HRF, −126 Da), and other fragments such as m/z 577 and 289 as a result of loss of (epi)catechin units, referring on previous MS data (Montero, Herrero, Ibáñez, & Cifuentes, 2013) these compounds were characterized as (epi)catechin trimers. Likewise, peaks $4–4_a–4_b–4_c–4_d-4_e - 4_f – 4_g–4_h–4_i–4_l$ (rt 37.96, 38.04, 38.70, 39.29, 39.31, 39.33, 39.42, 39.43, 39.74, 40.08, 40.19) were identified as (epi)catechin tetramers. Fragmentation pattern of peaks $5–5_a–5_b–5_c–5_d-5_e - 5_f – 5_g – 5_h$ (rt 41.70–41.74–42.33–42.40–42.47-43.12-43.21-43.87-44.0) were characterized by multiple loss of 289 Da, resulting from consecutive (QM) cleavages between the flavan units, according to previous Q-TOF data on apple procyanidins (Montero, Herrero, Ibáñez, & Cifuentes, 2013) these compounds were proposed as (epi)catechin pentamers. In a similar manner, peaks $6–6_a–6_b–6_c–6_d-6_e - 6_f – 6_g–6_h–6_i–6_l$ (rt 44.76, 44.80, 44.83, 45.42, 45.47, 45.49, 45.54, 46.16, 46.24, 46.89, 46.99) were tentatively

assigned as (epi)- catechin hexamers. Parent ions from tetramers to heptamer were all detected as doubly charged $[M-2H]^{2-}$. Peaks $7–7_a–7_b–7_c–7_d-7_e - 7_f – 7_g$ (rt 47.80 48.45, 48.50, 48.54, 49.14, 49.23, 49.24, 50.00) were identified as (epi)- catechin eptamer. Peaks $8–8_a–8_b–8_c–8_d-8_e$ (rt 50.09, 51.53, 52.32, 53.02, 53.07, 53.12) showed the MS/MS fragment ions at m/z 1008.2047, 863.1777 and 575.1144, which could result from HRF and from the consecutive QM cleavage of flavan units respectively, whereas fragments at m/z 737.1054 and 449.0860 are the products of a phloroglucinol loss (126 Da) from fragments at m/z 863 and 575 respectively. By these information, together with Orbitrap–MS spectra comparison in literature (Lin, Sun, Chen, Monagas, & Harnly, 2014), these compounds were tentatively identified as epi(catechin) octamers (DP 8). Increasing the retention, peak areas decrease (Kelm et al., 2006) and after oligomers with DP 8, two peaks $9 - 9_a - 10$ (rt 54.58, 55.30, 56.12) were observed. Two different MS signals were detected, even if their intensity was low, MS/MS and fragmentation pattern led to their tentative identification as oligomers with DP 9 and 10 which were detected as $[M-2H]^{2-}$ and $[M-2H]^{3-}$ respectively.

Supplementary References

Fromm, M., Loos, H.M., Bayha, S., Carle, R., & Kammerer, D.R. (2013). Recovery and characterisation of coloured phenolic preparations from apple seeds. Food Chemistry, 136, 1277–1287.

Ramirez-Ambrosi, M., Abad-Garcia, B., Viloria-Bernal,M., Garmon-Lobato, S., Berrueta, L.A., & Gallo, B. (2013). A new ultrahigh performance liquid chromatography with diode array detection coupled to electrospray ionization and quadrupole time-of-flight mass spectrometry analytical strategy for fast analysis and improved characterization of phenolic compounds in apple products. Journal of Chromatography A, 1316, 78–91.

Alonso-Salces, R.M., Ndjoko, K., Queiroz, E.F., Ioset, J.R., Hostettmann, K., Berrueta, L.A., et al. (2004). On-line characterisation of apple polyphenols by liquid chromatography coupled with mass spectrometry and ultraviolet absorbance detection. Journal of Chromatography A, 1046(1–2), 89–100.

Reis, S.F., Rai, D.K., & Abu-Ghannam, N. (2012). Water at room temperature as a solvent for the extraction of apple pomace phenolic compounds. Food Chemistry, 135,
1991–1998.
Fromm, M., Bayha, S., Carle, R., & Kammerer, D.R. (2012). Characterization and quantitation of low and high molecular weight phenolic compounds in apple seeds. Journal
of Agricultural and Food Chemistry, 60(5), 1232–1242
Garcia-Beneytez, E., Cabello, F.L., & Revilla, E.J. (2003). Analysis of grape and wine anthocyanins by HPLC–MS. Journal of Agricultural and Food Chemistry, 51, 5622–5629.

Sun, J., Lin, L.Z., & Chen, P. (2012). Study of the mass spectrometric behaviors of anthocyanins in negative ionization mode and its applications for characterization of anthocyanins
and non-anthocyanin polyphenols. Rapid Communications in Mass Spectrometry, 26, 1123–1133.

Oszmianski, J., Wojdylo, A., Gorzelany, J., & Kapusta, I. (2011). Identification and characterization of low molecular weight polyphenols in berry leaf extracts by HPLC–DAD and LC–ESI/MS. Journal of Agricultural and Food Chemistry, 59, 12830–12835.

Kalili, K.M., & de Villiers, A. (2009). Off-line comprehensive 2-dimensional hydrophilic interaction × reversed phase liquid chromatography analysis of procyanidins. Journal of Chromatography A, 1216(35), 6274–6284.

Sommella, E., Pepe, G., Pagano, F., Tenore, G.C., Dugo, P., Manfra, M., et al. (2013). Ultra high performance liquid chromatography with ion-trap TOF-MS for the fast characterization of flavonoids in Citrus bergamia juice. Journal of Separation Science, 36(20), 3351–3355.

Schieber, A., Conrad, J., Beifuss, U., & Carle, R. (2002). Elution order of Quercetin glycosides from apple pomace extracts on a new HPLC stationary phase with hydrophilic endcapping. Journal of Separation Science, 25(5–6), 361–364.

Porter, E.A., Van den Bos, A.A., Kite, G.C., Veitch, N.C., & Simmonds, M.S.J. (2012). Flavonol glycosides acylated with 3-hydroxy-3-methylglutaric acid as systematic characters in Rosa. Phytochemistry, 81, 90–96.

Schieber, A., Keller, P., Streker, P., Klaiber, I., & Carle, R. (2002). Detection of isorhamnetin glycosides in extracts of apples (Malus domestica cv. “Brettacher”) by HPLC–PDA and HPLC–APCI-MS/MS. Phytochemical Analysis, 13, 87–94.

Alonso-Salces, R.M., Ndjoko, K., Queiroz, E.F., Ioset, J.R., Hostettmann, K., Berrueta, L.A., et al. (2004). On-line characterisation of apple polyphenols by liquid chromatography coupled with mass spectrometry and ultraviolet absorbance detection. Journal of Chromatography A, 1046(1–2), 89–100.

Mari, A., Tedesco, I., Nappo, A., Russo, G.L., Malorni, A., & Carbone, V. (2010). Phenolic compound characterisation and antiproliferative activity of “Annurca” apple, a southern Italian cultivar. Food Chemistry, 123(1), 157–164.

March, R.E., & Miao, X.S. (2004). A fragmentation study of kaempferol using electrospray quadrupole time-of-flight mass spectrometry at high mass resolution. International Journal of Mass Spectrometry, 231, 157–167.

Sanchez-Rabaneda, F., Jauregui, O., Lamuela-Ravento's, R.M., Viladomat, F., Bastida, J., & Codina, C. (2004). Qualitative analysis of phenolic compounds in apple pomace using liquid chromatography coupled to mass spectrometry in tandem mode. Rapid Communications in Mass Spectrometry, 18, 553–563.

Montero, L., Herrero, M., Ibáñez, E., & Cifuentes, A. (2013). Profiling of phenolic compounds fromdifferent apple varieties using comprehensive two-dimensional liquid chromatography. Journal of Chromatography A, 1313, 275–283.

Lin, L.Z., Sun, J., Chen, P., Monagas, M.J., & Harnly, J.M. (2014). UHPLC–PDA–ESI/HRMSn profiling method to identify and quantify oligomeric proanthocyanidins in plant products. Journal of Agricultural and Food Chemistry, 62(39), 9387–9400.

Kelm, M.A., Johnson, J.C., Robbins, R.J., Hammerstone, J.F., & Schmitz, H.H. (2006). Highperformance liquid chromatography separation and purification of cacao (Theobroma cacao L.) procyanidins according to degree of polymerization using a diol stationary phase. Journal of Agricultural and Food Chemistry, 54, 1571–1576.